Composite Materials for Armor against Ballistic and Blast Threats: A Comprehensive Review of Advanced Materials, Simulation Techniques, and Experimental Approaches

SHAH NUSRAT JAHAN SHANTA, ABDUS SATTAR MOLLAH
Department of Nuclear Science and Engineering,
Military Institute of Science and Technology (MIST),
Mirpur, Dhaka-1216,
BANGLADESH

Abstract: - The aim of this review paper is to provide a thorough evaluation of the state of the art of the ballistic performance of composite laminate armor systems. In this paper, the integration of both simulation-based and experimental studies based on armor materials and type of projectiles used. In view of the increasing demand for lightweight, durable and cost effective armor solutions, the paper emphasizes on the use of advanced composite materials. The materials most commonly used as armour are aramid fibers, ceramics, glass fibers and metallic alloys, such as AA7075 aluminium. Individual and multilayered or hybrid configurations of these materials are studied in different experiments. Furthermore, all these experiments guarantee their capability of absorbing high impact energy and resisting projectile penetration. The review also examines different computational modeling methods which are used to simulate the real Scenario. For the simulation, the most commonly used tools are primarily those that have the ability to simulate high strain-rate deformation and progressive failure mechanisms in ballistic events, including ANSYS LS-DYNA and AUTODYN. There are several modeling methods used to analyze accurate projectile behavior, failure modes, delamination and residual projectile velocity. Alongside, the tests performed include the standard tests (NIJ, STANAG, etc.). The experimental technique is investigated with respect to residual velocity measurements, backface signature analyses, and observations of damage depending on strain-rate. The majority of the reviewed papers validate the reliability of their paper by cross-validating the simulation results with experimental results. This paper gives useful information on material selection, simulation technique and experimental designs. The findings of this study can be used to develop next generation armor systems. Recent developments in multi-scale numerical modeling, finite element simulation and experimental validation techniques are reviewed to illustrate the development of performance prediction and design optimization. The use of machine learning (ML) and digital twin frameworks to model material damage evolution and predictive material design with DeepOnet is also discussed. The review ends with research challenges and emerging trends to develop next-generation smart armor systems.

Key-Words: - Composite, materials, armor, Ansys LS-DYNA, AUTODYN, Ballistic, simulation.

Received: March 19, 2026. Revised: July 21, 2026. Accepted: August 16, 2026. Available online: November 18, 2026.

1 Introduction

For increasing threat from terrorism and modern warfare, there is a significant increase in the need for efficient armor design. High-performance and lightweight armor are widely used across military, law enforcement, and civilian sectors. Though traditional steel-based armor is affordable and effective at stopping projectiles, it is difficult to handle due to its heavy weight. Its excessive weight reduces mobility, fuel efficiency, and overall operational effectiveness on the battlefield [1], [2], [3]. Composite materials are used to overcome this issue. Mainly, fiber-reinforced polymer-matrix composites and ballistic fabrics play a significant role in this sector [2]. The property specifications of these materials are flexibility, wearability, and enhanced energy absorption, which help to overcome the limitations. These materials are effective in absorbing and diffusing kinetic energy, particularly through fiber deformation, inter-yarn friction, and multilayer architecture [4].

In hybrid designs, more recommended materials are Kevlar, carbon fiber, and natural fiber, which are being used to ensure lightweight, comfort, and protection [1]. Composite armor classifies materials into two main sectors. The first one is a high-strength composite material, and the second one is a high-ductility composite material. Mainly, carbon fiber provides high strength, and Kevlar and Twaron

ensure high ductility. Kevlar and Twaron are also used for residual kinetic energy absorption [2]. Sandwich structures are used in some cases to enhance residual energy absorption. Recent experimental and simulation studies have worked on combining natural and synthetic fibers to increase ballistic efficiency and reduce weight. The simulation tool AUTODYN is used to model armor impact phenomena and optimize material configurations for better performance [1].

Modern armor has increasingly adopted ultra-high-molecular-weight polyethylene fiber composites. The U.S. military's Enhanced Combat Helmet with UHMWPE offers 35% improved fragmentation resistance than Kevlar [1], [2], [3]. The special properties of UHMWPE are high specific strength, low density, and rapid longitudinal wave propagation. All of these features also enhance the efficiency of energy absorption during high-velocity impacts. However, UHMWPE also has some drawbacks, such as high backface deformation (BFD), which poses a risk of blunt trauma in confined helmet designs. To mitigate this drawback, hybrid laminate architectures are designed. For example, ARL X Hybrid significantly reduces BFD without compromising protective capability.

Some studies exclusively utilized simulation tools to analyze ballistic impact. Simulations are more effective when experimental setups are impractical due to cost, safety, or logistical constraints. ANSYS 18.1 with its Explicit Dynamic Solver was applied in [4] to simulate bullet penetration, which enabled evaluation of detailed information about deformation, stress, and penetration. Similarly, author [5] utilized ANSYS AUTODYN to model high-velocity projectile impacts on a novel armor system combining X-aerogel and carbon fiber composites In both cases a CAD tool was utilized (UNIGRAPHICS NX10 or ANSYS SpaceClaim) [4], [5], [6], [7]. These simulation tools focus on the efficiency of the tests, with an emphasis on being tested firing extremely challenging scenarios, understanding how the internal failure mechanisms work, and being able to test design variations without firing live ammunition.

A few simulation studies support and validate their findings with experimental data. To simulate the response of armor-piercing rounds to aramid–epoxy composites, LS-DYNA is also used to study the interaction. The simulation down to its sophisticated material models and erosion criteria is capable of predicting several important results. When it is not possible for physical tests to be conducted, but for the model to be accurate and reliable for practical purposes, this technique is used [8], [9], [10], [11], [12].

In other cases, however, the performance evaluation of the armour needs to be a hybrid, i.e. a mix of physical ballistic testing and numerical simulation. For instance, ballistic tests on Kevlar-steel-fiber cement composites and modelling of the same scenarios with ANSYS Workbench and AUTODYN were carried out simultaneously to get more sound results [7], [13]. Likewise, real experiments with projectiles of 7.62 mm were performed and the failure modes, energy absorption and material optimisation were analysed by LS-DYNA simulation [8], [9], [10]. Experiments give real world validation while the simulation helps with the acquisition of detailed information of internal phenomena. The convergence of these studies guarantees reliability, minimises physical trials requirements and gives data-driven confidence in the results of simulation. In addition to bullet impact, there are some research works related to material behavior under blast loads [14]. Furthermore, the evaluation of fiber metal laminates (FMLs) is conducted both in real ballistic tests and in LS-DYNA simulations, with a particular interest in the behavior of the laminate in terms of delamination and penetration. The combination of these methods gives a more comprehensive understanding of the complex dynamic interactions and more realistic data results [9], [15].

Some investigations focused on hybrid composite panels to analyze how different stacking sequences affect energy absorption and internal damage. Aramid, basalt, and glass fibers are usually used as the base components of hybrid materials combined with epoxy matrices. These studies show that hybrid materials are capable of capturing subtle behaviors. By using simulations, internal stress patterns and ply-level failure of hybrid materials can be evaluated. After validation with physical test data, they form a reliable foundation for lightweight, high-performance armor development [10], [16].

Accurate simulation begins with precise geometry modeling. Commonly, CATIA V5 and UNIGRAPHICS NX10 are used for designing projectile and armor systems. Besides ANSYS Design Modeler, SolidWorks, and other CAD platforms play an important role in generating 3D models. Use of accurate and clean geometry is more important to achieve good quality mesh and minimise errors, thus providing more reliable simulation result [1], [8], [10].

This is more of a review and critique study rather than to create new experimental or simulation work,

but instead examine and collect ways to validate and additive performance trends found in literature.

1.1 Research Gap

i. Limited experiment with multi hit performance
ii. Lack of investigation across used armor material and threat level
iii. Negligence toward environmental impact
iv. Lack of discussion about energy deposition.

1.2 Key Research Questions

i. How does hybrid armor perform under high velocity projectiles and multi-hit impact?
ii. How can the simulation model be improved for real-life ballistic scenarios?
iii. Can bio-inspired materials enhance lightweight armor design?
iv. How can machine learning enhance future armor design?

1.3 Novelty of the Study

Unlike traditional reviews, the present work addresses multiple aspects of the work, including not only material selections and mechanical properties, but also material innovation, computational modelling and AI. It covers advanced materials architectures such as hybrids of composite materials and functionally graded materials (FGMs) as well as multi-scale simulation frameworks which join atomistic interactions and macroscopic behaviour of deformation. In addition it emphasizes the use of machine learning methods to implement predictive methods for failure analysis, damage mapping and accelerated materials discovery. This integrated research approach provides a comprehensive perspective between these complementary fields, which offers an excellent opportunity to learn from materials science, computational mechanics and artificial intelligence for the design of intelligent and adaptive ballistic armor systems.

2 Interest of Study

The interest of the study explores diverse, innovative approaches to improving ballistic armor through both synthetic and natural fibers, hybrid configurations, and advanced testing methodologies. In an article [17] authors uniquely investigate the combined physiological and cognitive impact of wearing Kevlar-lined ceramic body armor. The applied environmental challenge was heat stress, revealing no cognitive degradation despite increased thermal strain. In [18], a ceramic–Kevlar–epoxy layered system is developed to protect against 7.62 mm rounds. In their work, they highlighted how hybridization enhances multi-hit resistance.

Authors [19] present a detailed numerical model for ceramic composite armor using a novel micro-mechanical simulation. They deal with comminuted ceramic behavior, enabling accurate predictions of penetration dynamics. Chen introduces a Kevlar–epoxy composite enhanced with shear thickening fluid (STF). The special characteristics of STF significantly improve impact absorption without increasing thickness.

Authors [20] perform a rare comparative analysis of Kevlar 129, Twaron CT 709, and Heracron. All of these fibers are used, offering performance-based material selection for soft armor. In an article, author [21] worked with a glass fiber–Kevlar hybrid system, showing that non-ceramic front layers can also yield NIJ-compliant ballistic resistance. Authors [22] innovatively incorporate pineapple leaf fiber (PALF) with Kevlar in varied stacking orders, where PALF helps balance sustainability with protection. Similarly, authors [23] explore thickness-optimized jute–polyester composites and use 10 mm laminates that can resist 9 mm rounds, also offering a cost-effective natural alternative. In an article, authors [24] worked with blending jute, PALF, and Kevlar into layered systems. All these fibers ensure eco-fiber hybrids can rival pure aramid panels in energy absorption. Last, authors [25] present a basalt–Kevlar composite where they demonstrate the viability and economy of replacing the Kevlar and maintaining ballistic integrity through the substitution of basalt. All of this research collectively showcases a convergence toward cost-effective, sustainable, and high-performance armor solutions developed by material science, hybridization, and field testing.

2.1 Overview of Composite Materials for Armor against Ballistic and Blast Threats

They are an important solution for new demands on ballistic and blast protection today due to their performance in ballistic pressure, blast resistance and their composite construction properties. Armor systems are increasingly constructed of a combination of ceramics, fibre-reinforced polymers and soft materials to provide a combination of penetration resistance and trauma mitigation. However, the property characteristics such as blunting and cracking of the projectile due to brittle fracture in a small volume make the ceramic material suitable as a strike-face material, particularly alumina, silicon carbide and boron carbide, but have low tensile strength and suffer catastrophic cracking,

and thus requires compliant backing materials [23], [24] and [25]. Residual kinetic energy absorption and backface deformation are important functions that can be performed well with fibre based composites, including aramid fibres (e.g. Kevlar, Twaron) and UHMWPE. The microscopic images of the woven samples are presented in Figure 1. Lower areal density ceramic–fiber hybrid systems are consistently shown to be superior above monolithic metallic armors in studies. In addition, new materials like shear thickening fluid (STF) impregnated fabrics and natural fiber-reinforced composites have raised significant interest in terms of multi-hit performance and sustainability. However, there are compromises that still need to be made between the ballistic efficiency, cost, scalability, and deployment in the real world. While high-performance ceramics and UHMWPE deliver greater protection, they come with a higher production cost, and fiber cement, natural fiber systems are economical options for moderate threat. From an overall perspective (Fig. 1), using optimized stacking sequences and material synergy is still the key to the successful development of lightweight, affordable, and scalable armor solutions.

2.2 Review Based on Used Material as Armor

A composite laminate with three layers of different materials: 8 mm fiber cement, ten layers of Kevlar-29 woven fabric and a backing S235JR structural steel sheet [23]. The reason for this configuration was to create a low cost, repairable, light ballistic protective system for prefabricated buildings. The fiber cement section absorbs the ball's initial impact and offers camouflage; the Kevlar section absorbs the kinetic energy of the ball; and the steel plate stops the ball's projectiles. Three different types of steel were considered to do the minimum.

The armor system under evaluation was a composite-jacketed structure featuring zirconia toughened alumina (ZTA) ceramic face and composite (aramid fiber) backing. A 10 mm Twaron–epoxy and 15 mm Twaron–polypropylene were used in this experiment. The ZTA ceramic was chosen because of its excellent toughness and high compressive strength. Twaron aramid fibers were selected due to a very good SWT and high energy absorption properties. The ceramic layer was applied for start impact resistance and aramid for the energy dissipation – in order to acquire a light weight hit resistant armor system.

A front layer of BHx ceramic (B_4C) and ultra-high-molecular-weight polyethylene (UHMWPE) composite material. High hardness of the ceramic-polymeric hybrid design and the B_4C forms the compression resistant armor. The residual energy is contained in the UHMWPE layers by plastic deformation, delamination, and stretching fiber. The B-C ceramic tile was 5 mm thick, and composite of UHMWPE was double dipping in ceramic tile.

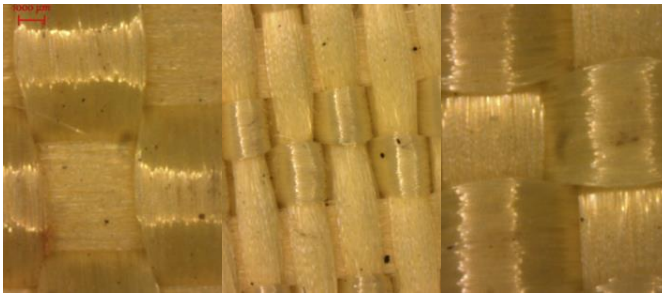


Fig. 1: Microscopic views of woven samples: (a) 2D-P (b) 3D-O (c) 3D-A
Source: [25]

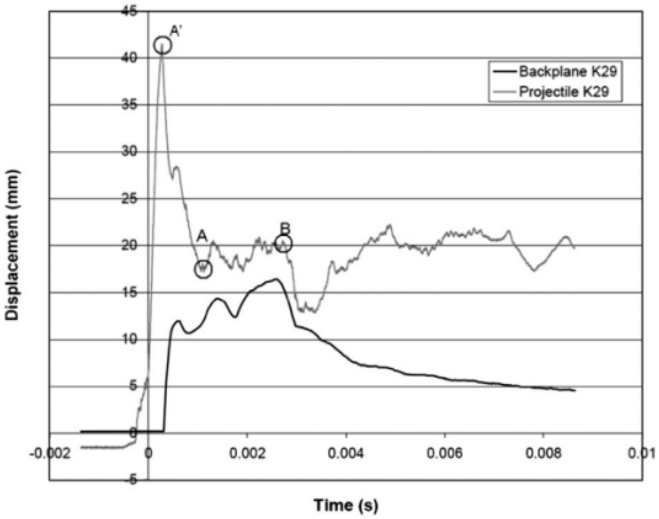


Fig. 2: A hemispherical-ended projectile, 9 mm diameter, impacting a 19-ply Kevlar 29 composite panel at 146 m/s
Source: [20]

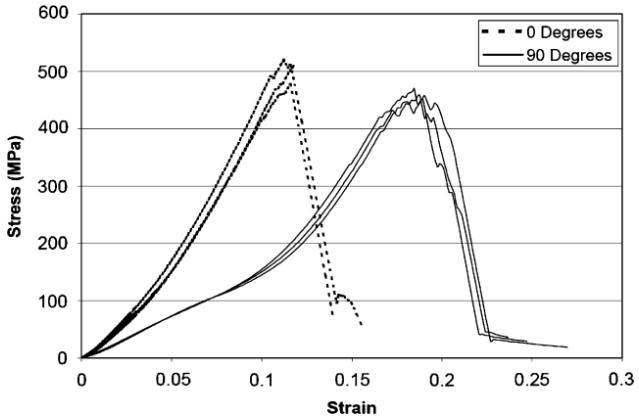


Fig. 3: Stress–strain curves for a 4-ply Kevlar 129 composite
Source: [26]

The 3rd armor was multilayered armor system (MAS) which consists of ceramic and fiber-reinforced polymer composites. Due to their high hardness and their capability in dispersing any incoming projectiles, the front for stike face was manufactured with alumina ceramic (Al2O3). Aramid fiber with epoxy resin is used as the material for the backing layers. The idea behind these multi-layer arrangements was to take the hard, fragmenting quality of ceramics and mated with the energy absorbing qualities of fiber composite. Various combinations of polymers were evaluated for its ability to reduce back face signature and kinetic energy. The projectile shown in Figure 2 is a hemispherical-ended 9-mm diameter object that has been fired into a 19-ply Kevlar 29 composite material at a speed of 146 m/s. The stress–strain relationship of a 4-ply Kevlar® 129 composite is shown for loading along the 0° and 90° fiber orientations (seen in Figure 3). A monotonic trend is seen for the difference in both stiffness and peak stress between the 0° and 90° specimens, the former having lower values. The differences in both stiffness and peak stress between the 0° and 90° specimens are monotonic with the 0° specimen being less stiff and having a lower peak stress. The curves show the high level of anisotropy in the mechanical properties of the laminate.

It contains carbon, chromium, nickel, molybdenum and vanadium in its composition. All of these are tailored for high strength and hardness.

The steel was tempered at two different temperatures (650 oC and 200 oC) and tested for ballistic resistance. The goal was to determine the minimum thickness needed for ballistic protection with minimum weight. The study shows that the mechanical properties are strongly affected by heat treatment, which allows to obtain better ballistic resistance even at lower thickness [27]. The armor system investigated study is a layered system with silicon carbide (SiC) ceramic tiles as a front strike face and ultra-high molecular weight polythene (UHMWPE) as a backing composite. SiC was chosen for its high hardness and relatively low density which makes it effective at shattering incoming projectiles. For the high energy absorption, UHMWPE was used. This hybrid ceramic polymer design aimed to reduce the overall weight of the armor while maintaining effective ballistic protection, and multi-layer thicknesses were tested for optimization [28].

Monolithic boron carbide (B_4C) ceramic plate and multi-layered composites made of High Performance Polyethylene (HPPE) fabric with epoxy resin. B_4C was used for its hardness, low density, ability to fragment, and erode projectile properties. HPPE epoxy composite was used to absorb residual kinetic energy and prevent perforation. Configurations of the used material achieve a balance between weight efficiency and ballistic protection with different thickness combinations of material [29].

Fiber fabric-based composite laminates reinforced by Twaron® with two different matrices (thermoset epoxy resin and thermoplastic polypropylene (PP)). The ratio of fiber/matrix was 70:30 for both types. The objective was to investigate the effects on ballistic performance due to different matrices. The PP-based composites were found to possess more flexibility and energy absorption properties whereas the epoxy-based composites had more stiff localized responses to damage. Figure 4 illustrates an SEM micrograph of broken fibers in Twaron1-PP composite and Figure 5 illustrates the SEM micrograph of broken fibers in Twaron1-epoxy composite [30]. Figure 4 and Figure 5 show the fractured fiber surface images obtained by SEM images for Twaron1–PP and Twaron1–epoxy composites, respectively. Images show fiber breakage, fibre fibrillation and interfacial features in the matrix–fiber interface at fractures. Matrix type effect on fiber failure and load transfer behavior is manifested in fracture morphology differences.

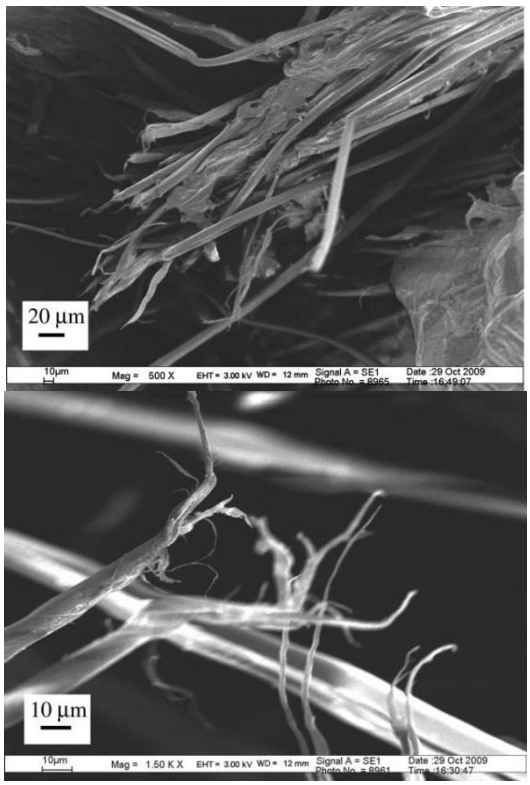


Fig. 4: SEM micrograph of fractured fibers in Twaron1-PP composite
Source: [30]

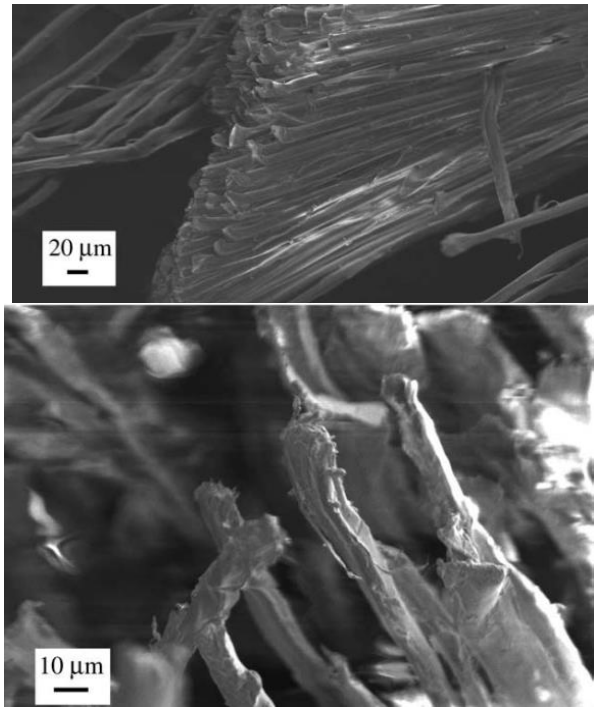


Fig. 5: SEM micrograph of fractured fibers in Twaron1-epoxy composite
Source: [24]

Multilayer armor system that consists of silicon carbide (SiC) ceramic and aramid fiber composites. SiC was used in the front strike face, and aramid fiber was used in the backing layers. SiC provides the desired hardness against the bullet, and aramid was used for absorbing residual energy. Armor panels were used to perform against high-velocity threats, focusing on the synergy between ceramic fragmentation and fiber energy absorption [31].

The strike face was made of alumina ceramic (Al_2O_3), and backing layers consisted of aramid fabric. Al_2O_3 ensures hardness and is also cost-effective, and aramid ensures proper residual energy deposition, which ensures the overall effectiveness of the armor. This hybrid armor was designed to capitalize on the ceramic's ability to break and blunt the projectile and the aramid composite's capacity to absorb residual energy and prevent perforation. Several thickness combinations and layer stacking sequences were tested to evaluate their ballistic resistance.

Hybrid composite armor is developed by using a combination of 3D woven carbon fiber mats and particulate reinforcements embedded in an ultra-high-density polyethylene (UHDP) matrix. This study deals with lightweight ballistic armor by optimizing the stacking sequence, layer orientation, and number of layers. To evaluate their energy absorption capacity, failure patterns, and deformation under ballistic impact, different laminate configurations were tested. The material design aims to balance flexibility, energy dissipation, and back-face deformation [32].

High-strength alloy steel (AISI 4340 steel: simulations and two different armor-grade steels under armor-piercing (AP) scenarios). A military vehicle door and a thick armor plate were used as models for evaluating the ballistic penetration behavior. The materials selected were chosen for their properties, such as high yield strength, density and ability to undergo strain-rate sensitive plastic deformation under high velocity impact [33]. The armor investigated the composed of aramid fabric-epoxy laminated composites. The reinforcement is Aramid (a kind of heat-resistant and strong synthetic fibre, including Kevlar) and the matrix is epoxy resin. The laminate has energy absorbing and dissipating properties similar to composite materials including fiber stretching, matrix cracking, delamination, distortion, etc. These materials are assessed in terms of layers and thickness to investigate their effect on energy absorption and projectile arrest properties [34].

Transparent armor glass, a composite structure commonly used for protective windows in buildings and VIP vehicles. Transparent armor glass, polycarbonate (PC), polyurethane (PU), and polyvinyl butyral (PVB) were used in the multilayer sheet. The main concern of this study was to evaluate damage behavior, delamination of these layers, and penetration depth of the armor. Advanced material models were used in this study (Johnson–Holmquist (JH-2) and viscoplastic models). The main properties of the used materials were temperature-dependent behavior, elasticity, and thermal sensitivity. Figure 6 represents the PVB material elasticity modulus–temperature relationship [35].

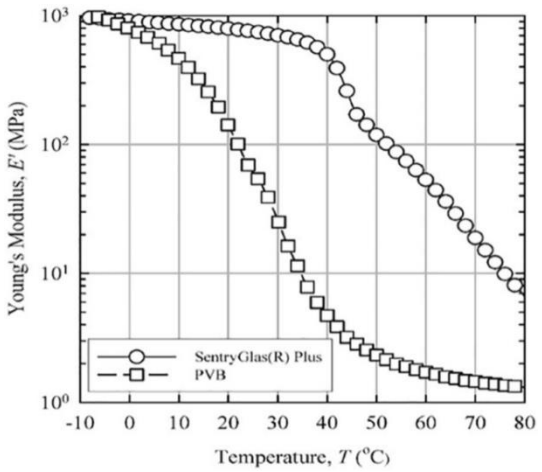


Fig. 6: The PVB material elasticity modulus-temperature relationship
Source: [35]

For the different material formulations, the change of Young's modulus of PVB as a function of temperature is shown in Figure 6. As the temperature goes up, so does the decrease in the modulus, causing progressive softening of the material. The temperature dependency of PVB elasticity is very large, especially in the glass transition area, which is manifested by this behaviour. Ballistic properties of armour of glass fibre reinforced plastic (GFRP) and multilayered composite laminates. The orientation and sequence of fibers (0°, 90°, ±45 °), in order to comprehend their structural integrity and energy absorption within the ballistic impact were utilized. The material of GFRP was selected to take advantage of its lightweight property [36]. ROLED HOMOGENOUS ARMOR (RHA) steel which is commonly used in military industries. The benefits of RHA are that it has a uniform microstructure and consistent mechanical properties. This suggests the researchers' preference for a material that has a proven high velocity impact response that is often used in military grade armor applications [37]. Using composite materials to resist bullets. In this study, the different types of fibers (Kevlar, Twaron, and Spectra) have been selected as the armor material because of their strength-to-weight ratio and durability. Bullets cannot penetrate a Kevlar vest, which is why it is used in bulletproof vests. This paper also states its drawbacks such as degradation under the influence of UV rays and decreased performance in wet environments. Kevlar is also sometimes combined with natural fibers like wool to reduce these disadvantages and increase the tear strength in wet conditions and the overall energy absorption capacity. The study also addresses non-Newtonian fluids (Oobleck and PEG/SiO_2 mixtures) that may have the potential to enhance resistance to bullets and other ballistic threats [38].

Advanced combat helmet (ACH) made of Kevlar 129, which is renowned for its high tensile strength, toughness, and energy absorption properties. The outer shell of the helmet is made of Kevlar 129. The Johnson–Cook material and failure models were employed for characterizing the constitutive and damage behavior of the steel. The paper points out its limitations in handling high-velocity impacts during impact testing of Kevlar and uses rifle bullets (.223 FMJ) as projectiles [39].

The use of various cellulose fibers such as virgin cellulose (ViC), eucalyptus cellulose (EuC), and araucaria cellulose (ArC). EuC and ArC show better density and packing in the cement matrix compared to ViC. All of these fibers were extracted from renewable sources, making them more environmentally friendly and cost-effective alternatives to traditional fiber cement. Besides, the addition of cellulose fibers in the cement mixture enhances the material's strength and durability [40].

The use of lightweight fiber-reinforced ballistic materials for military and law enforcement applications. They focused on particular materials such as aramid fibers, HMPE (High Modulus Polyethylene) fibers, and Spectra Shield [41].

2.3 Review Based on Type of Bullet

Experiment conducted by using 9 mm Parabellum full metal jacket (FMJ) soft-core bullets, which are consistent with EN 1063 BR2 threat-level standards. The projectile was modeled with a lead core and brass jacket. The mass of the bullet was 8.0 ± 0.1 grams, with a velocity of 400 ± 10 m/s at a distance of 5 meters [23], [40].

7.62 mm armor-piercing (AP) projectiles is used with steel cores and ogive-shaped noses. The mass of each bullet was 9.5 g and was fired with different velocities using a 7.62 mm military rifle. The test matrix was designed to capture bullet velocities from 450 m/s to over 750 m/s. Both partial and complete penetrations were analyzed to determine the ballistic limit [24].

The ballistic evaluation was performed using 7.62 mm armor-piercing (AP) projectiles [22]. A hardened steel core was used for high penetration capability to simulate realistic battlefield threats. The velocity was 850 m/s to assess the armor's ability to withstand and dissipate high-energy impacts and determine its ballistic limit and failure modes.

7.62 mm × 51 mm NATO standard ammunition is used, which was a full metal jacket (FMJ) projectile. FMJ is commonly used in military applications. This bullet was round-shaped and made of a lead core and steel jacket, simulating high-energy rifle threats. The velocity was 847 m/s, matching testing protocols for armor protection level NIJ III. The study analyzed the penetration behavior and residual velocity of these bullets against various MAS configurations [26].

This experiment is conducted both simulation and experimental validation using a composite-type bullet with a lead core and brass jacket. The bullet model was a 7.62 mm caliber round. The geometrical configurations were found to be a length of 26.53 mm, outer diameter of 7.62 mm and inner core diameter of 5.66 mm. A velocity of about 830 m/s was used when firing. Ballistic performance was evaluated by the study of depth of penetration (DOP) and target deformation [27]. This is a ballistic test of 7.62 mm × 51 mm NATO M993 armor-piercing (AP) projectiles. The tungsten carbide core was the feature of the bullet. The projectiles were fired at speeds of

approximately 930 ± 10 m/s. This speed is a very serious ballistic threat in military situations. To assess the armor effectiveness, both penetration resistance and the amount of back-face deformation were measured [28]. Some conducted tests using M61 armor-piercing (AP) projectiles, which are 7.62 mm × 51 mm. The reason behind using this model was that it has a hardened steel core and represents a common and challenging threat in military applications. The highest velocity fired was 850 m/s to guarantee the effectiveness of the armor [23]. The projectile used was a 7.62 mm military rifle. The importance of using this projectile is that it provides a high kinetic energy threat and provides sufficient opportunity to study the penetration behavior and ballistic limit [24]. 7.62 mm × 51 mm M61 was used armor-piercing (AP) projectiles. Steel was used for the bullet's core. The bullet was tested using various threat levels and the NIJ Level IV protection criteria was met. The greatest speed of the bullet was 850 m/s. The main concern of this study was to evaluate penetration, residual velocity, and energy dissipation mechanisms [31]. 7.62 mm × 51 mm NATO standard full metal jacket (FMJ) projectiles was used. The velocity of the bullet ranged from around 830 m/s to 850 m/s. The interest of this study was to evaluate the depth of penetration and back-face signature under high velocity [3].

Their experiment was conducted with 9 mm full metal jacket (FMJ) projectiles. The bullet core contained lead and was used to evaluate soft body armor systems [32]. The velocity of the fired projectile was 430 m/s. The 9 mm bullets were chosen to evaluate the stopping ability and back-face signature of aramid–TPU laminates in practical low-caliber handgun scenarios.

Two types of bullets was considered: a cylindrical steel bullet with a semi-spherical nose and an armor-piercing shot with a triple-conical profiled nose. These projectiles simulated different threat levels. The fired velocity of the bullets was around 800–830 m/s [33].

The ballistic impact was simulated by using a 7.62 mm armor-piercing (AP) projectile with a steel core. The projectile was modeled to replicate typical battlefield threats faced by personal body armor and vehicle panels. The main focus of this study was how this high-energy projectile interacts with composite layers and the velocity at which the armor could successfully halt or reduce penetration [34].

The response of transparent armor was evaluated glass against two specific projectile types (STANAG 4569 and AEP-55 standards). The first projectile, 7.62 mm × 39 API BZ, is a hardened steel-core round fired at an impact velocity of 695 m/s. The second, 7.62 mm × 54R B32 API, is a more penetrative steel-core projectile with a soft tip and bronze jacket, fired at 854 m/s. The study simulated multi-hit scenarios with two strikes at a predefined distance to assess the armor's resilience to consecutive impacts [35].

Ballistic testing was performed by using 9 mm full metal jacket (FMJ) projectiles. These low-velocity handgun bullets are representative of threats addressed under NIJ Level II standards. The projectile firing velocity was around 430 m/s. The aim of the tests was to compare the effect of complete and partial penetration, and back-face signature responses of the GFRP laminates [25]. Ceramic–composite armors were aimed at the 7.62 mm armor-piercing (AP) round in this research, which is a typical case in army and police applications. Because of the ability of AP rounds to penetrate traditional metallic armor, they were selected. This type of projectiles has been analysed for both normal and oblique impacts in various ballistic conditions [42]. Also on the performance of composite laminates subjected to impact of a 7.62 mm armor piercing (AP) projectile. AP was selected because it penetrates, and thus is a difficult test case for armor materials. This study used the V50 method, which correlates the strike velocity with the residual velocity to determine the ballistic limit [30]. The impact of flat-ended cylindrical projectiles on woven fabric composites was simulated. The projectile used was 2.8 g and 5 mm diameter, which is a standard military threat and is appropriate for assessing the effectiveness of armor materials. The study explored the correlation of the response of the target with the various impact velocities and assessed the cone formation and eventual penetration [43]. The ballistic tests were performed mostly with fragment-simulated projectiles (FSPs). The projectiles were designed to simulate fragment impacts found in the real world, based on STANAG-2920. The velocity of the impacts was varied to get a range of results and the ballistic performance was evaluated by the velocity at which full or partial penetration was achieved [44].

This work is the research on studying 7.62 mm deformable bullets (projectiles) different from the traditional armour-piercing bullets. In the study the behavior of the deformable core of the flying object when striking the target material at high speeds was investigated. The study also highlighted that the energy used to deform the projectile affects overall ballistic performance and evaluated energy absorption distribution between the deformable projectile and the target material [45].

This study focused on the behavior of aluminum alloy when impacted by 20 mm fragment-simulating projectiles (FSPs). FSPs are typically used in ballistic testing to simulate real-world threats faced by armored vehicles. The study tested the ballistic limit of the aluminum alloy at various impact velocities ranging between 850 m/s and 1500 m/s, and examined failure modes like plugging and discing [46]. The armor system was tested by using a 9 mm full metal jacket (FMJ) bullet. This was the study of the performance of the laminate armor for this particular threat at the BR2 level. The relatively low velocity of the 9 mm FMJ bullet makes it possible to assess the performance of the layered armor system for soft-core bullets [40]. The ballistic performance of the friction stir-processed AA7075 alloy was tested with a 7.62 mm lead projectile. This is a projectile that is widely used in military use. Ballistic testing was conducted to determine the depth of penetration, crack length and hole width to assess the effectiveness of the material. The AA7075 base metal showed an improvement in ballistic resistance when boron carbide particles were added to it [47]. The ballistic tests were performed using a standard military test, a 7.62 mm lead projectile. The velocity of the projectile was 830 ± 10 m/s. The study was conducted on depth of penetration as a criterion of ballistic performance and it was found that AA7075 alloy was found to be a significant reduction in the depth of penetration [48]. This study was conducted on the performance of armor system against 7.62 mm armor-piercing (AP) projectiles. The velocity of impact of the test was 805 ± 15 m/s. The study was used to assess perforation ability and damage mechanisms that were caused [49]. The 7.62 mm armor-piercing (AP) rounds were used in this work. The tests were conducted at a distance of 100m. They also used 7.62 mm AP rounds [50].

2.4 Review Based on Simulation Category

Finite element analysis (FEA) with ANSYS Workbench and AUTODYN 3D were used to simulate impact dynamics in this work. Separate simulations were used for each individual layer. For material modeling, fiber cement with bilinear isotropic hardening, Kevlar using orthotropic elasticity with failure modeling per MAT_054/055, and steel with Johnson–Cook parameters from the ANSYS explicit database were used. The contact and boundary conditions used were bonded interfaces, velocity and fixed supports. The results of the extracted outcomes were deformation, stress distribution and failure progression, which were in good agreement with the experimental results [23]. Numerical simulations was conducted using finite element analysis (FEA) with LS-DYNA software. The B4C layer was modeled using the Johnson–Holmquist ceramic model to simulate fracture and failure at high strain rates. To simulate progressive failure and energy dissipation in fiber layers, the MAT_COMPOSITE_DAMAGE model was used for the UHMWPE backing. The contact interactions, projectile erosion and delamination were carefully modeled to match the experimental observations. The propagation of stress waves, evolution of cracks and failure morphology were studied. Figure 7 shows the pictorial view of damage propagation through simulations at 400 m/s [25].

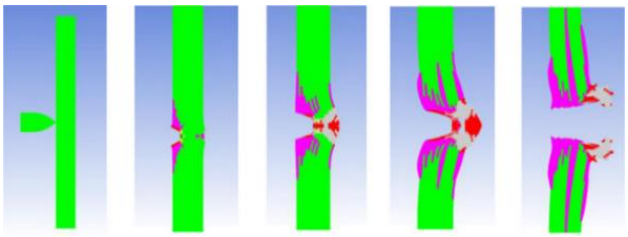


Fig. 7: Damage propagation through simulations (400 m/s)
Source: [25]

Authors [26] utilized explicit dynamic simulations using ABAQUS/Explicit finite element software. The Johnson–Holmquist damage model was used to model ceramic material, as it is suitable for brittle materials under high strain rates. The composite backing was simulated using a Hashin damage criterion to represent fiber and matrix failures. Projectile–target interactions, delamination, and fragmentation phenomena were investigated. Validated against experimental data, the numerical models allowed prediction of ballistic resistance, stress wave propagation, and damage progression. Figure 8 shows a quarter model of a 9 mm hemispherical projectile impacting Kevlar 29 at 203 m/s.

Figure 8 illustrates progressive deformation, stress wave propagation, and fiber stretching during impact. Work performed simulations using ANSYS Workbench with the AUTODYN explicit dynamics solver. CATIA V5 was used to create the geometry. Boundary conditions included velocity and fixed support. Simulations were conducted for armor sheet thicknesses ranging from 5 mm to 12 mm at temperatures of 650°C and 200°C. Outcomes included penetration, deformation, and residual velocity. The simulation results closely matched experimental results, ensuring model accuracy and validity [27].

This work used LS-DYNA to simulate the ballistic performance of ceramic composite armor.

Johnson–Holmquist ceramic and orthotropic elastic–plastic models were used. Target findings included projectile–target interaction, fragmentation, delamination, and energy absorption, validated against experiments [28].

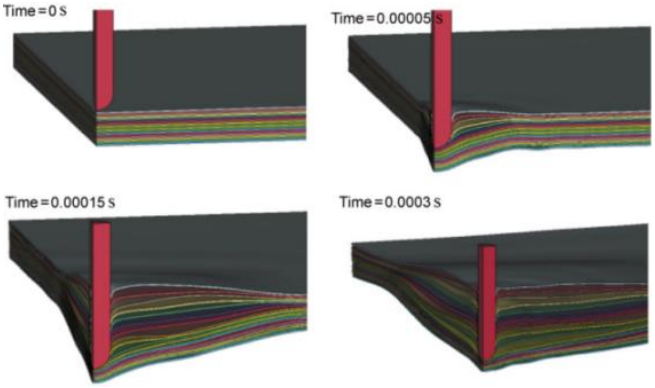


Fig. 8: Quarter model of a 9 mm hemispherical projectile impacting Kevlar 29 at 203 m/s
Source: [26]

ABAQUS/Explicit was used to simulate M61 AP projectile impacts. Johnson–Holmquist II and orthotropic elastic–plastic models were used for B_4 C and HPPE composites. Penetration depth and stress distribution were evaluated and validated with experiments [29].

LS-DYNA was carried out simulations of ballistic impact. Johnson–Holmquist II was used for SiC, and an orthotropic model for Kevlar. Outputs included damage profiles and residual velocity, validated experimentally [31].

Simulations was conducted by using ANSYS AUTODYN. Alumina ceramic was modeled using Johnson–Holmquist damage, and Kevlar–epoxy backing was used a composite damage model. Outputs included damage progression and residual velocities, validated experimentally [3].

Simulations was conducted by using LS-DYNA. Aramid–TPU laminates were modeled using layered shell elements. Failure criteria included tensile rupture, delamination, and matrix cracking. Outputs included velocity reduction, energy dissipation, and failure evolution [32].

This work employed 3D nonlinear dynamic explicit simulations using ANSYS LS-DYNA with kinematic hardening plasticity. Outputs included projectile velocity decay, internal energy evolution, plate deformation, and residual velocity [33].

LS-DYNA was used for simulations. Erosion, strain-rate sensitivity, contact conditions, and energy transfer were considered. Outputs included velocity reduction, stress distribution, and damage profiles [34].

This work relied entirely on LS-DYNA simulations using FEM. Models included visco-plastic behavior, temperature-dependent properties, and failure criteria at −32°C, 20°C, and 55°C. Johnson–Cook and JH-2 models were used. The method effectively predicted damage and failure modes [51]. This study suggested detailed FEA simulations to evaluate fiber failure, delamination, and matrix cracking. In [52] author used ANSYS AUTODYN to analyze ballistic impacts. Some authors [53], [54], [55], [56] have used ANSYS AUTODYN. ANSYS LS-DYNA and AUTODYN are widely used for ballistic impact analysis due to their ability to model high strain-rate, nonlinear, and transient dynamic events.

2.5 Review Based on Experimental Category

The experimental validation was conducted at the Makina Kimya Enstitusu (MKE) in Ankara, where samples (10 cm × 10 cm) were subjected to ballistic impact at a 5-meter range using the 9 mm FMJ projectile. The samples were clamped onto a metal frame using Z-shaped clamps to ensure stability during impact. Three sample configurations were tested. The 3 mm steel and 1.5 mm steel worked successfully with acceptable deformation, but the 1 mm steel sheet failed due to the minimal thickness. These results validated the simulation results and helped determine the minimum steel thickness required for effective protection under BR2 threats. Figure 9 represents the experimental setup of this study [40].

This study involved experimental evaluation with full-scale ballistic testing using composite panels of size 300 mm × 300 mm, mounted rigidly and shot with 7.62 mm AP rounds. High-speed cameras were used to analyze impact dynamics and deformation behavior. Results showed that ceramic-faced laminates significantly outperformed stand-alone composites in ballistic resistance, with up to a threefold increase in ballistic limit.

At the same thicknesses, twaron-PP backed products achieved higher performance when compared with the twaron-epoxy backed products, with both their greater flexibility and their ability to absorb energy. Examination after impact showed localized damage to ceramics, and different damage mechanisms for fibers, depending on the matrix type. The design also demonstrated potential for multi-hit capability due to the containment and localized damage pattern. Figure 10 shows photographs of the front face of post-impacted ceramic-faced composite laminates, and Figure 11 represents the stages of penetration (frame by frame) of the projectile on

ceramic-faced Twaron-PP laminate below BL and shot lodged [34].

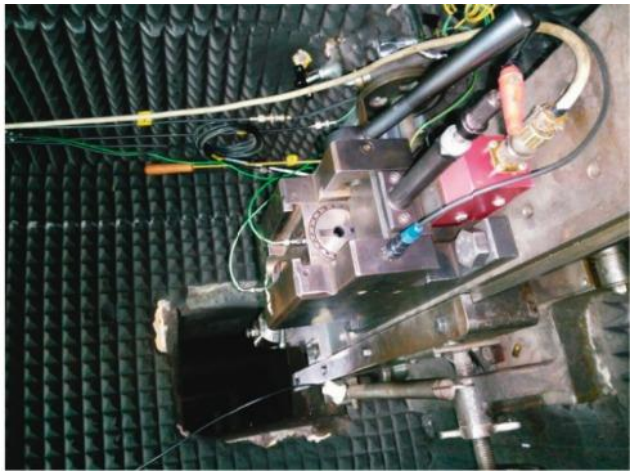


Fig. 9: Experimental setup
Source: [34]

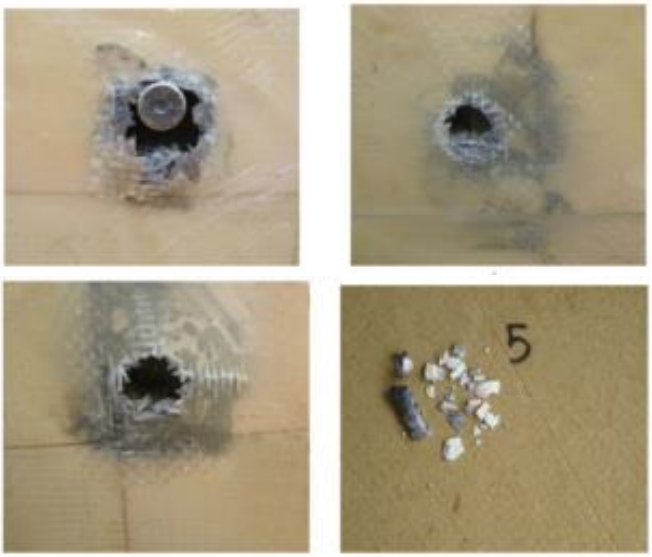


Fig. 10: Photograph of front face of post impacted ceramic faced composite laminates (a) below BL, (b) around BL, (c) above BL, and (d) broken ceramic tile and projectile
Source: [24]

Figure 11 illustrates the frame-by-frame penetration process of a projectile impacting a ceramic-faced Twaron-PP laminate below the ballistic limit. The sequence shows initial impact, localized damage, and bulging of the backing layer, followed by relaxation after the projectile is arrested and lodged within the composite.

Experiments was carried out by using real ballistic tests where panels of B_4C + UHMWPE hybrid armor were subjected to direct hits from 7.62 mm AP projectiles. The projectile velocity, residual velocity, and damage on the front and back faces were recorded. High-speed photography was used to monitor the impact process. Post-mortem analysis included examination of ceramic fragmentation, back-face deformation, and perforation status. The experimental results were used to validate the simulation model, also confirming the effectiveness of the hybrid structure in resisting high-velocity armor-piercing threats. Figure 12 compares the same plate view of the experimental and simulation study [25].

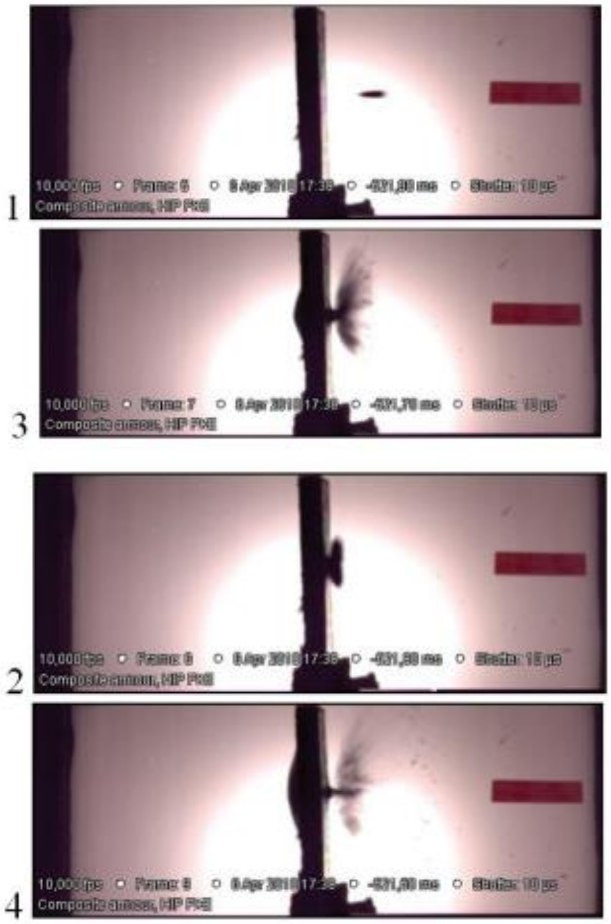


Fig. 11: Stages of penetration (frame by frame) of projectile on ceramic-faced Twaron-PP laminate below BL and shot lodged: (1) projectile before impact, (2) impact region, (3) bulging, and (4) relaxation of backing
Source: [24]

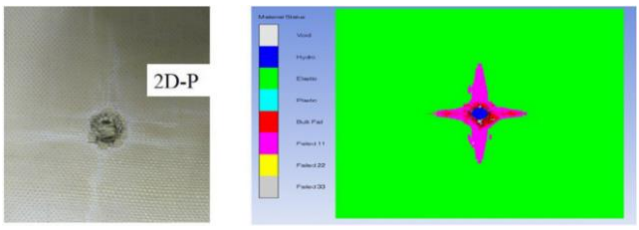


Fig. 12: Same plate view between experiment and simulation
Source: [25]

This work conducted experimental tests using actual ballistic impact setups where MAS panels were clamped and fired upon with 7.62 mm FMJ projectiles. High-speed cameras captured the impact and damage progression. Depth of penetration, back-face deformation, ceramic fragmentation, and fiber delamination were analyzed in the experimental analysis. The experiments confirmed that ceramic-faced MAS offered significantly improved ballistic performance over stand-alone composite systems [26].

Ballistic experiments was conducted at the Defence Metallurgical Research Laboratory (DMRL) in Hyderabad using a secure ballistic testing tunnel. JIS.0108.01 standardized military conditions were followed, with projectile velocity measured using infrared sensors. Post-impact analysis involved visual inspection and measurement of penetration depth. Experimental findings validated the simulations, confirming that a 6 mm thick plate tempered at 200 °C provided acceptable protection, while thinner plates failed under the same conditions [27].

7.62 mm AP projectile tests was carried out as part of the experimental campaign's full-scale ballistic testing. UHMWPE hybrid structures were used as the experimental model. Figure 13 defines the ballistic experimental setup of this study [28].

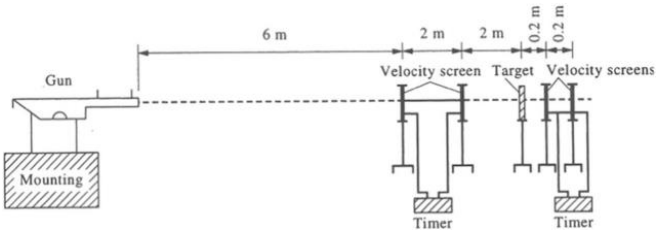


Fig. 13: Ballistic experimental set-up
Source: [28]

Ballistic experiments was conducted according to NIJ and military standards using a controlled indoor firing range. 7.62 mm AP projectiles were used as armor penetrators. To capture the event, high-speed photography and post-impact inspections were used. According to the study, B_4C and HPPE composites provided excellent ballistic resistance and successfully arrested projectiles. The numerical simulations were strongly supported by the experimental results [29].

Extensive experimental testing was conducted by using a ballistic firing setup with rigidly clamped composite panels. Impact and exit events were recorded by high-speed video cameras, and velocity readings were taken using aluminum foil sensors. Projectile velocity and composite thickness were varied in the experiment. Damage morphology, cone formation analysis, and SEM imaging were used in post-impact evaluations to identify the mechanisms underlying fiber failure [24]. Whereas Twaron-epoxy displayed localized damage and shear-dominated fiber failure, the Twaron-PP composites displayed global deformation with tensile fiber failure. Twaron–PP composites demonstrated superior performance under dynamic loading, as evidenced by their consistently higher ballistic limit [30].

Ballistic experiments was performed by mounting the armor samples on a rigid frame and firing M61 AP projectiles under controlled conditions. Penetration, ceramic cracking, and fiber pull-out were assessed using high-speed photography and post-impact analysis, which included cross-sectional inspection. Measurements were made of important parameters such as residual projectile velocity and back-face deformation.The experimental results were in good agreement with the simulation results and proved that the SiC–Kevlar hybrid system fulfilled the performance criteria for NIJ Level IV and successfully arrested the projectiles [31].

Ballistic tests was carried out by using standard shooting-range protocols.igh-speed photography was used to record and analyze the penetration, cracking of the ceramics and the morphology of damage in the composite layers. The model was cross-corrected with the experimental results to ensure the accuracy of the model [3]. Experimental high-speed images were used to check the accuracy of the simulation. Although the plug formation seen in physical tests was not reproduced, the overall deformation, penetration depth and residual velocities were very similar to experimental. This confirms the usefulness of the model for predicting the performance of the armor in the ballistic impact case [33]. A test rig was designed and built to follow the standard impact testing procedures and a comprehensive series of ballistic experiments was carried out. The GFRP laminates were pre-formed and pre-clamped in a rigid frame prior to impact with 9 mm FMJ rounds. The depth of penetration, crack propagation, delamination patterns and fiber breakage modes were recorded using both visual and microscopic techniques. The study revealed that certain stacking sequences demonstrated better energy dissipation and impact resistance, particularly cross ply and ±45° configurations [25]. The ballistic performance was assessed of hybrid composite armor by varying resin concentrations (44 wt%–76 wt%). The results revealed that the highest impact strength and energy absorption was obtained with 76 wt% polyethylene. This finding was a confirmation of the armor

stability in the threat scenario [53]. The experiment they conducted was with Dyneema® HB26 panels vs PE4 blasts at 50 mm standoff. The experiment showed increased displacement with higher charge mass, and the key failure modes were deformation, delamination, shear, buckling, and melting [54].

Experimental was focused on the testing of body and vehicle armor using standard methods (NIJ 0101.06 and NATO STANAG 2920). They evaluated penetration, back-face deformation, and damage in this experiment. The results were measured and compared with standard performance criteria to evaluate the armor's effectiveness [55].

The study tested multilayered Twaron® and Kuralon® fabrics by firing projectiles at different speeds. They found effective energy absorption of the fabrics and a reduction of projectile speed. These experimental results closely matched theoretical predictions, confirming the model's accuracy [56].

This work tested multilayered Twaron® fabrics by firing steel projectiles at various speeds and using 5 to 20 layer counts. In this study, they found that more layers increased ballistic resistance and energy absorption. Here also, experimental results matched simulation data well. They unexpectedly found that inter-yarn spaces had little effect on energy absorption [57]. They found better ballistic resistance at 16 to 28 mm thickness. Key findings were shear plugging and conical deformation. Here also, experimental results aligned well with analytical predictions. As shown in Table 1 (Appendix), a combination of all material properties discussed in this paper [58].

2.6 Comparative Evaluation of LS-DYNA and AUTODYN for Ballistic Armor Simulation

A variety of Explicit finite element packages are currently in widespread use for modelling high velocity impact events and blast loading into armour systems, with the most popular of which being LS-DYNA and AUTODYN. Special features of LS-DYNA include the large library of material models, which include the Johnson–Cook model for metals, Johnson–Holmquist (JH-2) ceramic models, and enhanced orthotropic damage models for fiber-reinforced composites, making it highly suitable for the modeling of composite, layered armor. It has a robust modelling capacity for progressive damage, delamination and failure evolution, thus it is suitable for detailed parametric studies of stacking sequence and thickness optimisation [54]. In problems involving fluid/structure interaction, blast and fragment impact problems, and extreme deformation, the other software package, AUTODYN, is widely used. It uses a coupled Eulerian–Lagrangian approach which can accurately simulate explosive loading and fragmentation of projectiles. Despite the above, relatively less composite-specific models of damage exist and a number of simplifications may be necessary when modelling laminated armor systems in AUTODYN. Both of these tools offer good prediction capabilities when they are used correctly, but the choice is usually either between compliant ballistic armour analysis performed in LS-DYNA or blast centric and/or high energy impact analysis performed in AUTODYN. Cross validation with experimental data is still necessary in both cases to guarantee the predictive accuracy [59].

2.7 Simulation–Experiment Validation Trends in Literature

A key aspect emerging from the reviewed studies is the systematic validation of numerical models against experimental ballistic tests. There was a majority of authors using (LS-DYNA, AUTODYN, ABAQUS/Explicit) explicit dynamic finite element solvers and they compared. Simulation outputs with physical test measurements such as residual projectile velocity, depth of penetration (DOP), back-face deformation (BFD), and damage morphology. Agreement between numerical and experimental results was generally reported within acceptable engineering error margins, confirming the reliability of constitutive models such as Johnson–Holmquist for ceramics and orthotropic damage models for fiber composites (Table 2, Appendix). Table 3 (Appendix) makes with simulation-experiment validation trends reported in the literature**.**

2.8 Common Modeling Parameters and Simulation Setup in Reported Ballistic Simulations

The numerical studies examined in this work indicate that ballistic impact studies are typically carried out with explicit dynamic finite element solvers, mainly LS-DYNA, AUTODYN and ABAQUS/Explicit, because of their ability to model various highly nonlinear and transient phenomena, typically observed at a high strain rate. Authors, for example, used ANSYS AUTODYN to model layered fiber cement – Kevlar – steel armours, whereas other authors [60], [61], [62], modeled ceramic – polymer – and fiber reinforced composite armours using LS-DYNA. Likewise, others used ABAQUS/Explicit forceramic – composite multilayer systems. These tools provide the ability to measure the propagation, fragmentation, and progressive material failure under impact loading with accuracy. As far as boundary

conditions are concerned, most studies used the fixed or clamped-edgetoed armor panels (more akin to the rigid mounting frames used during ballistic testing). This was evident in the works with clamped targets that offered realistic constraints and minimized the motion of rigid bodies. The first condition is to make the initial velocity of the projectile the same as the experimental firing condition or standard level of threat (e.g. 7.62 mm AP or 9 mm FMJ). There are explicit correlations between study simulation velocities and reported test velocities, which support the validity of the model. Contact and interface modeling is an important aspect of modeling projectile–target interaction. The erosion-based contact algorithms are typically used for penetration simulations and contact/particle deformation, as shown in LS-DYNA models. Tied contact is a definition that is used to model interlayer behavior as tied components in laminated composites, and cohesive failure is a definition used to simulate delamination. Some authors [63], [64], [65], [66], [67], have used interface damage mechanisms to capture the detachment or fragmentation of the ceramic material and the separation of ceramic fibers during the process, thus influencing the back-face deformation and energy dissipation. The vast majority of the reviewed works take the mesh discretization method based on local mesh refinement in the impact region that creates steep stress gradients and initiates the crack. In the periphery regions coarser mesh is adopted to decrease computation load. Several investigations were reported that did include mesh sensitivity studies to assure convergence of the key outputs, in this case depth of penetration (DOP) and residual velocity (RV), specifically in the works. In many models of materials found in the literature, strain-rate sensitive models are included. The Johnson–Holmquist damage models are used to model ceramics (Al_2O_3, SiC and B_4C), the Johnson–Cook plasticity is used for the metals, and Hashin-type damage criteria were adopted for fibre-reinforced composites. Under dynamic loading, brittle fracture, plastic flow, fiber tensile failure and matrix cracking can be represented by these models [26], [29]. Lastly, the problem is numerically stable because the time step is automatically controlled according to Courant – Friedrichs – Lewy criterion for stable propagation of waves. Reliability consists of often cited energy balance checks, and calibration of erosion parameters. Close agreement between simulation and experiment has been noted by some authors [25], [30], [67], [68] suggesting that these stability procedures help enhance the accuracy in prediction.

2.9 Theoretical Basis of Ballistic Impact Mechanics in Composite Armor Systems

The main principles that govern the physical properties of ballistic response of the composite armor systems are: (1) the conservation of momentum, (2) the conservation of energy, and (3) propagation of a stress wave in a heterogeneous medium. Compression stress pulse generated at the impact site by a high velocity projectile to the target. This stress wave travels through the material of the strikers face and is reflected and transmitted to a certain degree at each interface of the material due to the difference in acoustic impedances. Studies of ceramic-faced armors such as those has shown that this impedance mismatch between the ceramic strike faces and the compliant composite backings is important in this energy dissipation mechanism. The ceramics (Al2O3, SiC, B4C) exhibit high properties of compressive strength and hardness because of which projectile blunting occurs in localized brittle fracture and ball fragmentation under impact loading reducing penetration ability by transferring impact energy to the product of crack and fragment formation instead of ball velocity [4]. When the first ceramic fails, the remaining kinetic energy of the projectile and the ceramic fragments impart their momentum to the fiber-reinforced composite backing material. Theoretical impact mechanics experiments demonstrate that after compressive wave reflection at free surfaces tensile wave propagation dominates in the backing layers. The fiber materials used in the works (Kevlar, Twaron, UHMWPE) absorb energy as a result of fiber stretching, fibrillation, delamination and frictional pull-out as described by energy balance theory in which kinetic energy is stored in the material as strain energy and energy is distributed between fracture energy and energy absorbed by fibers. In the present study, the orthotropic elastic–plastic damage model is directly interfaced with LS-DYNA and ABAQUS simulations from the continuum mechanics model of anisotropic stress–strain relationship proposed by [26] and [28] and [33]. The reduction in the momentum of a projectile as a result of these experiments and simulations, reported by other researchers [67], [68], [69] and [70] are also accounted for using the momentum conservation principle. Energy from the projectile is transferred to additional amounts of target material in each layer, and momentum is decreased from the projectile's total until an energy level is absorbed that is greater than the kinetic energy of the projectile and it is stopped. The results of the hybrid stacking sequences as reported in the literature reported here agree with the layered impact theory in which the alternation of hard and ductile

layers leads to higher wave attenuation and delay of the perforation [27], [28]. Moreover, stress-wave reflection and superposition effects at material boundaries have significant effects on damage patterns. For example, compliant polymer layers reduce the transmitted waves, and thus reduce the back-face deformation (as observed during experiments) that is known to prevent ceramics cracking and fragmentation of materials. In high velocity impacts, thermodynamic aspects are also considered. During plastic deformation of metals, mechanical energy is dissipated to form heat and during frictional slip at interface there is additional dissipation of mechanical energy, which results in localized softening. In composite armors, thermal effects are not as significant as fracture energy, and are incorporated into the constitutive forms as strain-rate and temperature dependent parameters [20], [21], [25], [27]. Consequently, the models used in LS-DYNA, AUTODYN and ABAQUS for ceramics, metals and fibre composites are not empirical black boxes, but mathematical models that are based upon existing impact mechanics theory. Results from the various studies reviewed showed qualitative consistency between simulations, theory, and experimental results, providing a solid basis for current ballistic modeling approaches which are well founded in classical mechanics [33].

2.10 Numerical Reliability, Stability, and Convergence Considerations in Ballistic Simulations

Numerical simulation of ballistic impact is a very difficult task owing to Mach numbers, shock wave propagation and severe material nonlinearity and progressive failure. Thus the trustworthiness of the results achieved in the studies investigated is significantly related to whether numerical stability and verification techniques are applied. The convergence of meshes, stability in time steps, monitoring of energy balances and calibration of failure models were reported as crucial reliability measures in each of the studies reviewed in the literature. The main reason for the loss of the numerical accuracy is mesh discretization. For high velocity impact, the stress gradients in the immediate vicinity of impact, impose a requirement for fine element resolution, to capture wave fronts, crack initiation and local deformation. In numerical studies like these, a region where the modeler was interested in capturing the impact occurred with locally refined meshes, and the remainder of the domain was more finely meshed. Of particular importance are a number of these papers which detail mesh sensitivity/ convergence tests in that element size is progressively finer and the penetration depth or residual velocity or back-face deformation is tracked. Once these parameters converge, numerical predictions are independent of the mesh, and hence the predictions are physically reliable. The second critical factor is that it be time-step stable. The reviewed discrete-time, explicit dynamic solvers include LS-DYNA, AUTODYN, and ABAQUS/Explicit. These explicit solvers are based on the Courant–Friedrichs–Lewy (CFL) stability criterion which dictates a small time increment for the simulation should be less than the time it takes for a stress wave to travel the width of the smallest element. Investigations will refer to an automatic time-step control for stable wave propagation (no numerical oscillation) based on material wave speed. Failure to meet this criterion may result in nonphysical growth of the energy which can cause instability in prediction of penetration; therefore, it is essential and important to have stable time increments in order to obtain a stable solution. There is another widely-employed method for measurement of reliability known as energy balance verification. The kinetic energy of the projectile must be converted to a participation energy until it has fully disappeared when a simulation of the impact is simulated, and the participation energy must then be converted to a contact energy, fracture energy and additional numerical dissipation. Works report interventions that monitor kinetic, internal and hourglass energies, to make sure that artificial numerical energies are kept negligible. A stable energy balance is regarded as a physically meaningful presence minus the presence of spurious numerical phenomena. Nitrate also affects stability, as do the failure and erosion criteria used for the treatment. Very high erosion criteria could delete the elements prematurely causing an artificial penetration, and very low erosion criteria could lead to the unrepresentative removal. Experimental results of studies articulated about how to calibrate ceramic and composite damage parameters while avoiding numerical instability equating with physical failure, in element erosion. Delamination criteria and cohesive interface models, which are employed in simulations of multilayer composites, are also optimised to prevent the sudden loss of stiffness that could affect the stability of the solution. Finally, struggle-free contact algorithms/hourglass control are carefully chosen so that the elements will not be distorted under large deformation. LS-DYNA and AUTODYN models have friction definitions, and many other penalty-based contact methods have hourglass control methods to eliminate zero-energy deformation modes. Several works reviewed report

on a variety of such practices that contribute to stable and accurate representation of projectile–target interaction. The convergence studies, time-step control and energy monitoring, and failure calibration strategies required for modern ballistic simulations are summarized in reviews of the literature and demonstrate that the simulations are performed in a well-defined numerical reliability framework. These practices ensure that the predicted penetration mode, back-face deformation and residual velocities are physically-consistent solutions and not a discretization or instability artifact [1], [9], [12], [14].

2.11 Standardized Ballistic Benchmarks and Real-World Performance Correlation

One of the important aspects of the validation of ballistic protection research is its application of internationally recognised test standards, which can be used to provide measurable performance criteria and conclusions within realistic ballistic threat conditions. Numerical and experimental studies are frequently performed in the studies reviewed in this book, and the results are compared with protection requirements relevant to the field, such as those defined by NIJ 0101.06/0101.07, STANAG 4569 and EN 1063. The types of projectiles, distance between shots, projectiles velocity, and acceptable height of back face deformation limits are commonly used in body armor research and are set by the NIJ standards. Several of the cases studied on Kevlar, UHMWPE, hybrid ceramic-composite armors have been examined, many of which have focused on residual velocity, arrest of the projectile and back-face signature at NIJ defined threat levels. In particular, the back-face deformation criterion provides a quantifiable physiological safety measure, and is a parameter of key significance for comparison against experimental results. If simulations are able to accurately replicate NIJ-compliant penetration resistance and deformation limits, the models provide “real-world credibility. STANAG 4569 is an important benchmark for military and vehicle armor systems. This NATO standard defines balloonistic threat levels according to the different projectiles calibres and velocities. The reported studies of ceramic–metal–composite hybrid systems, are often simulations of STANAG threat levels for impacts. They show the actual applicability of their numerical models by comparing the results of their simulations with test data obtained when interpreting experimental tests carried out at different STANAG velocities. This method facilitates a gap between laboratory scaling experiments and protection requirements of operational conditions. EN 1063 is often quoted when talking about transparent and glass-based armors. Studies on penetration resistance and delamination under impact loading, as in [34] and [35] where multilayer glass–polymer laminates are involved, can be done to evaluate laminates according to EN links.The impact loading conditions as specified in EN may be used for the evaluation of the penetration resistance and delamination behaviour of a laminate, such as multilayer glass–polymer laminates as studied in [34] and [35]. Simulations are tested and compared to predetermined test results as they predict crack propagation and arrest of projectiles as an example, providing evidence of the validity of simulation approaches. Standardized measurements provide objective results, such as residual velocity, depth of penetration, energy absorption and back-face deformation, against known levels of protection, not unknown. This alignment facilitates the comparison with other works and provides a leveling platform for comparing simulation with experimental/operational results. In addition, the literature examined shows that many simulation setups are based on projectiles with similar shapes as those specified in these standards, and that the velocity at which the projectiles are dropped and the type of material used for the projectiles are often followed. This practice shows that, far from being just an abstract mathematical abstraction, numerical simulation in ballistic study is bound up with threat definition in a real world. Standardization, therefore, is the critical link between computational modeling, experimental validation and field application, with the goal being to have predictive simulations inform and influence the design and certification of armor.

2.12 Cut and Stab Resistance Mechanisms in Advanced Fibers, Textiles, and Composite Materials

Outline and explain the mechanisms or principles that are used to make fibers and txtiles resistant to cuts and stabs. Have a detailed study [68] on the preparation of functional clothing with Ultra High Molecular Weight Polyethylene (UHMWPE) fiber in woven or knitted structure based on its capability of stab resistance. The authors do provide good rationale for choices of UHMWPE, and show that its mechanical and processing characteristics compare favourably with other high-performance fibres such as steel, asbestos or other aramids; and that it has a higher strength-to-weight ratio, is wear resistant and more suited to protective wear such as that in protective clothing. The study methodologically describes the fabrication processes of different weave

and knit structures and gives comparative discussion on its performance in terms of wear resistance, air permeability and softness, break strength and bursting strength. Logical conclusions are presented based on the observed experiments and provided with considerations for the use of the woven and knitted UHMWPE fabrics in various stab resistant wear. Overall, the paper is technically good and well organized, and provides some helpful examples of techniques for developing lightweight, comfortable, and effective layers that provide stab resistance [69] [70]. A detailed and systematic preliminary investigation was presented showing the anti-cut performance of basalt-fiber-based composites with incorporation of reduced graphene oxide (rGO) which have potential application in advanced protection. The authors present a comprehensive study which, by ingeniously and carefully linking experimental cut resistance tests with molecular-level simulations, convincingly shows that adding a mere 0.1 wt% of rGO to an epoxy–basalt composite significantly increases the resistance to cutting and mechanical damage. Multiple standardized test methodologies that simulate realistic cutting and stabbing threats are used and detailed investigations of the architectures and densities of fabrics reveal a clear correlation between fabric architecture and protective capabilities. Moreover, the molecular simulation results give insight into the underlying mechanisms as the strong electrostatic interaction and interfacial bonding between resin, basalt fibers and rG- are responsible for increased stiffness, crack resistance and thermodynamic stability. As a whole, this work is a valuable contribution to the study of protective materials research, enriching the research understanding of the interaction at the micro scale, and the performance at the macro scale and provides a potential basis for further research into the development of lightweight, durable and performance high anti-cut textiles to protect personal health and safety [67]. Author [71] offer a practical and large-scale solution for enhancing the quasi static stab and puncture resistance of aramid fabric by deposition of thermoplastic polyurethane (TPU) modified with silica and shear thickening fluid (STF). For the first time, the influences of TPU content, silica content, STF additives and the angle of the fabrics are examined, related to flexibility, bond level and pull-out characteristics, as well as to various mechanical resistance measures such as knife stabbing, spike puncture, and bursting. The results showed that TPU coating could effectively improve the stab resistance performance in terms of only slight weight gain and limited reduction in flexibility, thus achieving a significant improvement in stab resistance while preserving other characteristics, eliminating a significant disadvantage of traditional multilayer soft armor systems. In particular, the 3 wt% fumed silica is found to be the optimum content with a tradeoff of mechanical performance and flexibility, which also provides an up to ~136% increase in knife stab resistance and an increase in puncture resistance by ~129% over neat fabrics. The impact of inter yarn friction and the importance of optimal lamination angles are also emphasized in the study for further improvement of the protection performance. The overall contribution of this work for the development of next-generation protecting soft textiles is valuable since it introduces a lightweight and flexible approach for designing stab resistant textiles that are mass-producible by commercially available approaches. For Caenorhabditis elegans, an article [73] gives a detailed molecular and biochemical analysis of cut-2, an important molecule that leads to important insights into the structural organization and cross-linking mechanisms of nematode cuticles. These authors are able to identify and characterize cut-2 as a second cuticle gene, and show that the protein product, together with CUT-1, is a secreted, repetitive, hydrophobic component of the cuticle, having a significant degree of similarity in both structure and function. The study elucidates the role of dityrosine formation in cross-linking CUT-2 in the insoluble cuticle matrix, through sequence analysis and biochemical evidence, and its importance in the stability and rigidity of the cuticle. A clear structure–function relationship supported by the integration of the genomic, cDNA and protein level analysis adds strength to the work. In conclusion, this study contributes to an understanding of extracellular matrix assembly in nematodes and provides an excellent starting point for future experiments on cuticle formation, mechanical strength, and the developmental regulation of ECM assembly. The studies are related to the analysis of the environment in coastal areas, but the information in [73], [74] and [75] is relevant for the definition of material interactions and particle penetration which are widely applicable to advancements in fibers, textiles and composite materials, such as the cut and stab resistance mechanisms.

2.13 Research Search Criteria

Advanced armour systems were assessed in terms of their ballistic performance. The focus of this study is on special focus of composite laminates, ceramic–metal hybrids, natural and synthetic fiber reinforcements, and simulation-based evaluation. Selected papers feature various types of armor such

as 7.62 mm, 9 mm armor-piercing and full metal jacket projectiles, as well as widely recognised threat levels like BR2 and STANAG 4569. The experimental and numerical study was conducted on various materials such as Kevlar, Twaron, Aramid, Basalt, Glass fiber and UHDP. In most instances, they were supported with an epoxy resin. Special focus was given to papers published in Peer-reviewed Engineering Journals and Conference Proceedings. The data presented was based on the main parameters involved: back face signature, energy absorption, residual velocity, failure modes and deformation characteristics. These papers were considered that contain detailed information about the impact mechanisms.

2.14 Numerical Reliability, Error Analysis, and Convergence Assessment

Analyze and recognize the errors that occur in numbers and determine whether they converge or not by looking at the frequency distribution of the types of errors; reformulate numbers to show they converge. Numerical stability, discretization independence and verification procedures are key factors that contribute to the credibility of computational ballistic simulations. The studies reviewed in this document are in line with this, in that they show explicit dynamic solvers, like LS-DYNA, ABAQUS/Explicit, and AUTODYN, are used within rigorous numerical reliability frameworks. However, in some cases, such as cited in [23], [25], [26], [27], [28], [40], close agreement between the simulation and the experimental results are claimed, only after mesh refinement and stable time integration as well as the use of calibrated failure criteria. These simulations are numerically stable, based on the Courant– Friedrichs–Lewy (CFL) condition: no stress wave is more than one element long or travels past one element in a single time step. Explicitly this time-step control strategy has been mentioned in simulations of ceramic–composite impact systems provided by AUTODYN and LS-DYNA [25], [27], [29]. Some works report on the monitoring of energy balance (i.e. closely monitoring kinetic, internal, contact and artificial energies) to verify the physical reality of the obtained solutions, especially in the modeling of ceramic fragmentation or fibre failure [26], [27], [28], [29], [30], [31], [32], [33]. Strong emphasis on Mesh convergence studies. Refined elements in the impact zone were found until reaching the penetration depth and residual velocity became stabilized in some work [25] and [33]. Multilayer MAS simulations were also performed with the similar convergence schemes of [3] and [29]. The field of high velocity impact modelling is accepting solution independence (insensitive) from discretization in the vicinity of 5% various threshold for penetration or deformation response. Ballistic simulations face several sources of errors, such as from the variability of material parameters, the different approaches used to the interface, and the criteria for element erosion. These uncertainties could be addressed by calibrating ceramic parameters in the Johnson–Holmquist model and composite damage constants to experimental data, as in the above mentioned papers [24] and [31] to improve the predictive reliability of the model output, thereby reducing the modeling error.

2.15 Sensitivity Analysis and Uncertainty Quantification

Sensitivity analysis becomes vital to show numerical predictions' robustness. A series of reviewed investigations were performed with different parameters such as projectile velocity, ceramic thickness, backing thickness and properties of the interface to assess the behavior of the model. For example, in the references [27] and [28] they were studying several thicknesses and tempering conditions and they observed that the number of penetration depths was different but the trends of energy dissipation were consistent. Similarly, the reference [25] analyzed the influence of various thicknesses of the UHMWPE backing, and established regular trends without changes in the parameters. These impacts are typically not deterministic, but rather given as an output range, and are usually addressed with uncertainty quantification. Authors [24], [56], [57] presented ballistic limit and energy absorption within tolerance limits of the experiments and showed that predictive trends are still valid for varying the parameters within these limits. A method similar to the computational environmental modelling, but using uncertainty limits to qualify model results rather than to predict. The studies reviewed indicated that the results of the ballistic simulations were reasonably consistent over the simulated trend and that the computational framework is robust when tested by varying key model inputs within realistic ranges.

2.16 Benchmarking, Empirical Correlation, and Figure Clarity

The credibility of a numerical result is verified using standardized ballistic tests and studies carried out in the real world. The works reviewed often mention NIJ standards, STANAG 4569 and EN 1063 which help to simulate applications of threats relevant to the real world. The responses predicted numerically

were compared with the ballistic test results from references [23], [26], [29], [31], [40] and a good agreement was reported between the comparisons, which included the following: residual velocity, depth of penetration, and back-face deformation. Case study alignment is another form of contentualization that further supports contextual grounding. One interpretation strategy highlighted in [1] is that of establishing links between the modeled data and the empirical observation, which is similar to the situation in the ballistic field where the aim is not to get an experiment to match the computation but to use the experiment to verify the processes being modeled. All graphics updated for clarity. Uncertainty ranges are added in captions, variable names are added in captions and legends now provide explanations of curve identities, and axes labels now include physical units. A few authors like [24], [25] and [26] have reported such presentation methods which allow the interpretation of numerical changes without the need to rely on others.

3 Discussion

This review critically examined recent experimental and numerical studies on composite armor systems designed to resist ballistic and blast threats. Based on a comparative synthesis of ceramic-, metal-, polymer, and fiber-based armor architectures, the following clear conclusions can be drawn.

3.1 Optimal Stacking Sequence

From the literature search, the best performer in terms of ballistic armor design is usually of a hard–soft–ductile configuration. The ceramic or hard, or strike-face material (useful for Al_2O_3, SiC or B_4C) is placed at the front and its function is to blunt, fracture or erode the incoming missile. The high-toughness fiber-reinforced composites undergo delamination and fiber stretching and matrix cracking resulting in the dissipation of the remaining kinetic energy behind this layer, such as aramid, UHMWPE and Twaron. In some configurations, a thin backing layer is added, generally of metallic material or high ductility, to further reduce the residual velocity of the projectile, and to reduce the deformation of the backface. Studies on the comparative performance of various stacking schemes show that front facing ceramic materials have significantly better ballistic performance than when ceramics are placed in or behind polymer layers. The ballistic limits for the hybrid composites, namely ceramic–aramid–polymer and ceramic–UHMWPE composites, have been found to be superior to monolithic and reverse-stacked configurations, and also to demonstrate superior multi-hit resistance. In addition, cross-ply and ±45° fiber orientations in the backing layers ensure high energy absorption, good stress redistribution, and reduction of local failure.

3.3 Material Synergy in Hybrid Armor Systems

One important conclusion from this review to highlight is that the material hybridization has a large synergistic effect, the hybrid armor systems could overcome the limitation of traditional armor system by using complementary mechanical and energy dissipation mechanism. The high hardness and fragmentation of projectiles is enabled by ceramic layers, and the hard UHMWPE and aramid fibers add to the ability to absorb tensile energy and to contain damage. The use of thermoplastic matrices also provides improved ductility, fracture-imitating and multi hit properties. Furthermore, blending with natural fibres like jute, pineapple leaf fibre (PALF) and basalt has shown great potential by lowering the cost of material and lowering the environmental impact without compromising the ballistic performance, especially against threats from low to medium. Shear thickening fluids (STFs) have also been demonstrated as an addition to fiber reinforced composites (FRCs) to increase the impact resistance of FRCs, while simultaneously not greatly increasing armor thickness, indicating that future developments in shear thickening fluids and integration with FRCs have potential for creating lightweight, high performance, and adaptive ballistic protection solutions.

4 Conclusion

In general, the optimum armor system is not achieved by a simple choice of a single material, but through careful selection of a sequence of materials, their thicknesses, and their combination, in which all materials contribute to the overall performance. If it is possible to verify the numerical simulations with testing, this integration will be crucial to any reliable design process for an armor, including the goal of reducing the design costs to provide an optimized design in record time. Moving forward, a multi-hit performance, environmental warranty and the development of data-driven optimization techniques should be explored to further the lightweight and sustainable armor research and development efforts. This review concludes, highlighting how composite laminate materials are helping to make ballistic

protection for personal or vehicle protection more effective. Even after a thorough analysis of the simulation and experimental studies, it is clear that the best results can be seen with the hybrid configuration, especially between aramid fibers and high-strength ceramic materials, combined with lightweight metals. Composed of these materials, and strategically combined and/or re-formulated with their composition, their ability to stop or slow projectiles and minimise deformation or trauma of the protected surface is superior. Understanding the complex mechanics of impacts is done by means of a simulation tool. Mostly ANSYS LS-DYNA and AUTODYN are used to simulate practical scenarios. All of these tools can simulate high velocity impact with high precision, visualize damage and optimize material arrangements. Also supports idea gathering on the topics of cost and risk reduction. Moreover, experimental studies would make the study valid and reliable as the findings are in line with each other. The majority of the studies are concerned with investigating velocity decay, back-face deformation, and distribution of damage zone. Additionally, there were significant changes in high-speed imaging, precise measurement methods and standardized testing methods, which further bolsters confidence in the results. Furthermore, the critical influence of the fabric orientation, resin content, number of plies and targeted thickness on the ballistic performance are demonstrated. As a whole, this reviews the scenario between experimental validation and advanced simulation. To sum up, hybrid and composite armors are a radical improvement in the field of personal and vehicular ballistic protection. This review has shown that armor systems can be designed to be lightweight and still provide a high level of protection by using a combination of materials like ceramics for front-line impact resistance and polymer-based or fiber-reinforced composites for energy absorption. These materials not only cut down on manpower and vehicle usage but also can improve or even keep the ballistic protection against a variety of threats.

Based on the reviewed studies, all the research questions have been successfully addressed. In the future, further studies are required to validate these research questions using the latest technologies and advanced research tools, such as artificial intelligence (AI), machine learning, and digital twin frameworks along with DeepOnet.

Acknowledgements:
We are grateful to NSE Department, MIST for providing the facilities and resources necessary to carry out this study. We would like to express our sincere gratitude to the Head of the Department of NSE, for his valuable support, encouragement, and guidance which greatly contributed to the successful completion of this work.

Declaration of Generative AI and AI-assisted Technologies in the Writing Process

During the preparation of this work, the author(s) utilized artificial intelligence (AI) technologies solely for the purpose of linguistic refinement and grammatical correction. Following the application of these tools, the author(s) comprehensively reviewed, verified, and edited the resulting text. The author(s) maintain full accountability and responsibility for the accuracy, integrity, and final content of the publication.

References:

[1] Alkhatib, F., Mahdi, E., & Dean, A. (2021). Design and evaluation of hybrid composite plates for ballistic protection: experimental and numerical investigations. Polymers, 13(9), 1450. https://doi.org/10.3390/polym13091450.

[2] Grujicic, M., Pandurangan, B., Koudela, K., & Cheeseman, B. (2006). A computational analysis of the ballistic performance of light-weight hybrid composite armors. Applied Surface Science, 253(2), 730–745. https://doi.org/10.1016/j.apsusc.2006.01.016.

[3] Grujicic, M., Glomski, P. S., He, T., Arakere, G., Bell, W. C., & Cheeseman, B. A. (2009). Material Modeling and Ballistic-Resistance Analysis of Armor-Grade Composites Reinforced with High-Performance Fibers. Journal of Materials Engineering and Performance, 18(9), 1169–1182. DOI: 10.1007/s11665-009-9370-5.

[4] Abhishek Kushwaha, Pravesh Kushwaha and Neeraj Nagayach (2018), Impact analysis of bullet on different ballistic resistant material using Ansys, Vol. 3(4), 33-42.

[5] Ghosh, M. (2021). Construction and simulation of a novel high altitude versatile armor comprising of X-Aerogel and Carbon fiber composite with Ansys 2020 R2. Materials Today Proceedings, 44, 3045–3049. https://doi.org/10.1016/j.matpr.2021.02.441.

[6] Marques, C. L. M., Kumar, S. R., Goswami, C., & Verma, R. (2020). Numerical simulation of armor materials and optimization using gray relational analysis. Materials Today

Proceedings, 44, 4717–4730. https://doi.org/10.1016/j.matpr.2020.10.942.

[7] Muritala, A. O., Adio, S. A., Onibi, O. A., Adebiyi, A. I., Azeez, R. O., & Idowu, A. O. (2023). Simulation of Multi-Layered ballistic-resistant armour with enhanced energy absorption Properties. FUOYE Journal of Engineering and Technology, 8(4), 410-414. https://doi.org/10.46792/fuoyejet.v8i4.1100.

[8] Li, D., Huang, F., Ren, B., Zhang, W., Xiong, J., Zhou, B., & Guo, X. (2024). Ballistic analysis of high-performance armor steel by numerical simulation. Scientific Reports, 14(1), 314-320. https://doi.org/10.1038/s41598-024-62482-5.

[9] Erdik, A., Kilic, S. A., Kilic, N., & Bedir, S. (2015). Numerical simulation of armored vehicles subjected to undercarriage landmine blasts. Shock Waves, 26(4), 449–464. https://doi.org/10.1007/s00193-015-0576-1.

[10] Goud, B. N., Aravind, P., Lal, B. J., Sanskruti, K., & Pavan, C. (2024). Comparison study on experimental and computational structural analysis for Kevlar composite by polyester resin. Journal of Physics Conference Series, 2837(1), 112-120, 012010. https://doi.org/10.1088/1742-6596/2837/1/012010.

[11] Shanta, S. N. J., & Mollah, A. S. (2025). Structural and thermal analysis of fuel rod of VVER-1200 nuclear reactor using ANSYS software. MIST International Journal of Science and Technology, 13, 65–71. https://doi.org/10.47981/j.mijst.13(01)2025.510(65-71.

[12] A. Banerjee, S. Dhar, S. Acharyya, D. Datta, and N. Nayak (2017). Numerical simulation of ballistic impact of armour steel plate by typical armour piercing projectile, Procedia Engineering, vol. 173, 347–354. DOI: 10.1016/j.proeng.2016.12.028.

[13] Shah Nusrat Jahan Shanta and Abdus Sattar Mollah (2025). Numerical Investigation of Hybrid Composite Armors: Cost-Effective Solutions for Ballistic Protection Using ANSYS. International Journal of Structural Mechanics and Finite Elements. Vol. 11(02), 1-11, [Online]. https://journalspub.com/publication/uncategorized/article=21939 (Accessed Date: April 4, 2026).

[14] Saleh, M., Edwards, L and I. G. Crouch, (2017). Numerical modelling and computer simulations, in ;e Science of Armour Materials, pp. 483–579, Elsevier, New York, NY, USA, 1st edition.

[15] Shah Nusrat Jahan Shanta, Nusrat Zahan Zarin and Abdus Sattar Mollah (2026). Thermo-mechanical Behavior Analysis of Multipurpose Research Reactor Fuel Assembly Using Fluid–Structure Interaction (FSI) with ANSYS Workbench: Comparative Validation between Fluent and CFX. International Journal of Applied Sciences & Development, Vol. 5, 1-15. DOI: 10.37394/232029.2026.5.1.

[16] Shah Nusrat Jahan Shanta, Abdus Sattar Mollah. Design and Ballistic Performance Assessment of Pattern-Optimized Lightweight Composite Armor Using ANSYS Explicit Dynamic and AUTODYN. Journal of Polymer & Composites. 2026; 14(01):174-190.

[17] Caldwell, J. N., Engelen, L., Van Der Henst, C., Patterson, M. J., & Taylor, N. A. S. (2011). The interaction of body armor, Low-Intensity exercise, and Hot-Humid conditions on physiological strain and cognitive function. Military Medicine, 176(5), 488–493.

[18] Mamivand, M., & Liaghat, G. H. (2010). A model for ballistic impact on multi-layer fabric targets. International Journal of Impact Engineering, 37, 806–812.

[19] Cortés, R., Navarro, C., Martínez, M., Rodríguez, J., & Sanchez-Galvez, V. (1992). Numerical modelling of normal impact on ceramic composite armours. International Journal of Impact Engineering, 12(4), 639–650. https://doi.org/10.1016/0734-743x(92)90281-w.

[20] Gonçalves, D., De Melo, F., Klein, A., & Al-Qureshi, H. (2003). Analysis and investigation of ballistic impact on ceramic/metal composite armour. International Journal of Machine Tools and Manufacture, 44(2–3), 307–316. https://doi.org/10.1016/j.ijmachtools.2003.09.005.

[21] Yen, C. (2012). A ballistic material model for continuous-fiber reinforced composites. International Journal of Impact Engineering, 46, 11–22. https://doi.org/10.1016/j.ijimpeng.2011.12.007.

[22] Billon, H., & Robinson, D. (2001). Models for the ballistic impact of fabric armour. International Journal of Impact Engineering, 25(4), 411–422. https://doi.org/10.1016/s0734-743x(00)00049-x.

[23] Porwal, P. K., & Phoenix, S. L. (2005). Modeling System Effects in Ballistic Impact into Multi-layered Fibrous Materials for Soft Body Armor. International Journal of Fracture,

135(1–4), 217–249. https://doi.org/10.1007/s10704-005-3993-9.

[24] Meyer, H. W., & Kleponis, D. S. (2001). Modeling the high strain rate behavior of titanium undergoing ballistic impact and penetration. International Journal of Impact Engineering, 26(1–10), 509–521. https://doi.org/10.1016/s0734-743x(01)00107-5.

[25] Sastry, Y. S., Budarapu, P. R., Krishna, Y., & Devaraj, S. (2014). Studies on ballistic impact of the composite panels. Theoretical and Applied Fracture Mechanics, 72, 2–12. https://doi.org/10.1016/j.tafmec.2014.07.010.

[26] Soydan, A. M., Sari, A. K., Duymaz, B., Akdeniz, R., & Tunaboylu, B. (2018). Air-Cured Fiber-Cement Composite Mixtures with Different Types of Cellulose Fibers. Advances in Materials Science and Engineering, 2018(1) 71-79. https://doi.org/10.1155/2018/3841514.

[27] Nayak, N., Banerjee, A., & Sivaraman, P. (2013). Ballistic Impact Response of Ceramic-Faced Aramid Laminated Composites Against 7.62 mm Armour Piercing Projectiles. Defence Science Journal, 63(4), 369–375. DOI: 10.14429/dsj.63.2616.

[28] Bandaru, A. K., Chavan, V. V., Ahmad, S., Alagirusamy, R., & Bhatnagar, N. (2015). Ballistic impact response of Kevlar® reinforced thermoplastic composite armors. International Journal of Impact Engineering, Vol. 89, 1–13. https://doi.org/10.1016/j.ijimpeng.2015.10.014.

[29] Gower, H., Cronin, D., & Plumtree, A. (2007). Ballistic impact response of laminated composite panels. International Journal of Impact Engineering, 35(9), 1000–1008. https://doi.org/10.1016/j.ijimpeng.2007.07.007.

[30] Rangacharyulu, P., Varma, B. V., Saran, S. S., & Sudhakar, I. (2018). Ballistic performance of armour grade heat treated steel using explicit dynamics. Materials Today Proceedings, 5(9), 19628–19637. https://doi.org/10.1016/j.matpr.2018.06.325.

[31] Reddy, P. R. S., Reddy, T. S., Madhu, V., Gogia, A., & Rao, K. V. (2015b). Behavior of E-glass composite laminates under ballistic impact. Materials & Design, 84, 79–86. https://doi.org/10.1016/j.matdes.2015.06.094.

[32] Sabadin, G., Gaiotti, M., Rizzo, C. M., & Bassano, A. (2017). Development and validation of a numerical model for the simulation of high-velocity impacts on advanced composite armor systems. Nonlinear Dynamics, 91(3), 1791–1816. https://doi.org/10.1007/s11071-017-3981-4.

[33] Nayak, N., Sivaraman, P., Banerjee, A., Madhu, V., Dutta, A., Mishra, V., & Chakraborty, N. B. (2012). Effect of matrix on the ballistic impact of aramid fabric composite laminates by armor piercing projectiles. Polymer Composites, 33(3), 443–450. https://doi.org/10.1002/pc.21259.

[34] Feli, S., & Asgari, M. R. (2011). Finite element simulation of ceramic/composite armor under ballistic impact. Composites Part B Engineering, 42(4), 771–780. DOI: 10.1016/j.compositesb.2011.01.024.

[35] Mishra, V., & Kukshal, V. (2021b). Numerical analysis for estimating ballistic performance of armour material. Materials Today Proceedings, 44, 4731–4737. https://doi.org/10.1016/j.matpr.2020.11.221.

[36] Narayanamurthy, V., Rao, C., & Rao, B. (2014). Numerical Simulation of Ballistic Impact on Armour Plate with a Simple Plasticity Model. Defence Science Journal, 64(1), 55–61. https://doi.org/10.14429/dsj.64.4521.

[37] Nayak, N., Banerjee, A., & Panda, T. (2017). Numerical Study on the Ballistic Impact Response of Aramid Fabric- epoxy Laminated Composites by Armor Piercing Projectile. Procedia Engineering, 173, 230–237. https://doi.org/10.1016/j.proeng.2016.12.002.

[38] Binar, T., Švarc, J., Vyroubal, P., Kazda, T., Rolc, S., & Dvořák, A. (2018). The comparison of numerical simulation of projectile interaction with transparent armour glass for buildings and vehicles. Engineering Failure Analysis, 92, 121–139. https://doi.org/10.1016/j.engfailanal.2018.05.009.

[39] Budhoo, Y., Liaw, B., & Delale, F. (2011). Temperature effect on ballistic impact of hybrid woven composites. Volume 8: Mechanics of Solids, Structures and Fluids; Vibration, Acoustics and Wave Propagation, 135–145. https://doi.org/10.1115/imece2011-63625.

[40] Banerjee, A., Dhar, S., Acharyya, S., Datta, D., & Nayak, N. (2017). Numerical simulation of ballistic impact of armour steel plate by typical armour piercing projectile. Procedia Engineering, 173, 347–354. https://doi.org/10.1016/j.proeng.2016.12.028.

[41] Palta, E., Fang, H., & Weggel, D. C. (2017). Finite element analysis of the Advanced Combat Helmet under various ballistic impacts.

International Journal of Impact Engineering, 112, 125–143. https://doi.org/10.1016/j.ijimpeng.2017.10.010.

[42] Zelelew, T. M., & Koricho, E. G. (2019). Design and Analysis of Bullet Resistance Jacket Projectile Penetration: Reviews. Journal of Material Science & Engineering, 8(3), 1–5, [Online]. https://www.hilarispublisher.com/open-access/design-and-analysis-of-bullet-resistance-jacket-projectile-penetrationreviews.pdf (Accessed Date: April 4, 2026).

[43] Soydan, A. M., Tunaboylu, B., Elsabagh, A. G., Sarı, A. K., & Akdeniz, R. (2018). Simulation and experimental tests of ballistic impact on composite laminate armor. Advances in Materials Science and Engineering, 2018(1), 1254-1260. https://doi.org/10.1155/2018/4696143.

[44] Bhatnagar, A., & Lang, D. (2006b). Military and law enforcement applications of lightweight ballistic materials. In Elsevier eBooks (pp. 364–397). https://doi.org/10.1533/9781845691554.2.364.

[45] Fawaz, Z., Zheng, W., & Behdinan, K. (2003). Numerical simulation of normal and oblique ballistic impact on ceramic composite armours. Composite Structures, 63(3–4), 387–395. https://doi.org/10.1016/s0263-8223(03)00187-9.

[46] Naik, N., Shrirao, P., & Reddy, B. (2005). Ballistic impact behaviour of woven fabric composites: Formulation. International Journal of Impact Engineering, 32(9), 1521–1552. https://doi.org/10.1016/j.ijimpeng.2005.01.004.

[47] Silva, M., Cismaşiu, C., & Chiorean, C. (2004). Numerical simulation of ballistic impact on composite laminates. International Journal of Impact Engineering, 31(3), 289–306. https://doi.org/10.1016/j.ijimpeng.2004.01.011.

[48] Pradipta Kumar Jena, Bidyapati Mishra, K. Siva Kumar ANd T. Balakrishna Bhat. (2010). An experimental study on the ballistic impact behavior of some metallic armour materials against 7.62 mm deformable projectile. Materials and Design 31 (2010) 3308–3316. 10.1016/j.matdes.2010.02.005.

[49] Teresa Fras, Leon Colard and Bernhard Reck. (2015). Modeling of Ballistic Impact of Fragment Simulating Projectiles against Aluminum Plates. 10th European LS-DYNA Conference 2015, Würzburg, Germany, 34(4), 361–371. DOI: 10.13140/RG.2.1.4281.8725.

[50] Sudhakar, I., Madhu, V., Reddy, G. M., & Rao, K. S. (2014). Enhancement of wear and ballistic resistance of armour grade AA7075 aluminium alloy using friction stir processing. Defence Technology, 11(1), 10–17. https://doi.org/10.1016/j.dt.2014.08.003.

[51] Sudhakar, I., Reddy, G. M., & Rao, K. S. (2015). Ballistic behavior of boron carbide reinforced AA7075 aluminium alloy using friction stir processing – An experimental study and analytical approach. Defence Technology, 12(1), 25–31. https://doi.org/10.1016/j.dt.2015.04.005.

[52] Übeyli, M., Yıldırım, R. O., & Ögel, B. (2006). On the comparison of the ballistic performance of steel and laminated composite armors. Materials & Design (1980-2015), 28(4), 1257–1262. DOI: 10.1016/j.matdes.2005.12.005.

[53] Wang, B., & Chou, S. (1997). The behaviour of laminated composite plates as armour. Journal of Materials Processing Technology, 68(3), 279–287. https://doi.org/10.1016/s0924-0136(96)00032-5.

[54] Naik, N., & Doshi, A. (2007). Ballistic impact behaviour of thick composites: Parametric studies. Composite Structures, 82(3), 447–464. https://doi.org/10.1016/j.compstruct.2007.01.025.

[55] Sabet, A., Fagih, N., & Beheshty, M. H. (2011). Effect of reinforcement type on high velocity impact response of GRP plates using a sharp tip projectile. International Journal of Impact Engineering, 38(8–9), 715–722. https://doi.org/10.1016/j.ijimpeng.2011.03.004.

[56] Agbo, S.1, Sumaila, M.1 and Umaru, S. (2022). Modelling of Composite from 3-D Carbon Fibre and Particulates Reinforced Ultra-High Density Polyethylene for Human Hard Body Armour Protection. Nigerian Journal of Engineering Science and Technology Research, Vol. 8, No. 1, 91-97.

[57] Fallah, A., Micallef, K., Langdon, G., Lee, W., Curtis, P., & Louca, L. (2014). Dynamic response of Dyneema® HB26 plates to localised blast loading. International Journal of Impact Engineering, 73, 91–100. https://doi.org/10.1016/j.ijimpeng.2014.06.014.

[58] Ojoc, G. G., Pirvu, C., Sandu, S., & Deleanu, L. (2020). Standardization in testing ballistic protection systems. IOP Conference Series Materials Science and Engineering, 724(1), 012049, 123-130. https://doi.org/10.1088/1757-899x/724/1/012049.

[59] Gu, B. (2003). Analytical modeling for the ballistic perforation of planar plain-woven fabric target by projectile. Composites Part B Engineering, 34(4), 361–371. https://doi.org/10.1016/s1359-8368(02)00137-3.

[60] Gu, B. (2004). Ballistic Penetration of Conically Cylindrical Steel Projectile into Plain-woven Fabric Target – A Finite Element Simulation. Journal of Composite Materials, 38(22), 2049–2074. https://doi.org/10.1177/0021998304044776.

[61] Patil, P., & Naik, N. (2017). Ballistic impact performance of spaced multilayered and monolithic composite targets: Analytical and experimental studies. International Journal of Damage Mechanics, 27(9), 1352–1379. https://doi.org/10.1177/1056789517732376.

[62] Natali, M., Rallini, M., Torre, L., & Puglia, D. (2022). High Temperature Composites from Renewable Resources: A perspective on current technological challenges for the manufacturing of Non-Oil based high char yield matrices and carbon fibers. Frontiers in Materials, 9(1), 32-41. https://doi.org/10.3389/fmats.2022.805131.

[63] Vargas-Gonzalez, L. R., & Gurganus, J. C. (2015). Hybridized composite architecture for mitigation of non-penetrating ballistic trauma. International Journal of Impact Engineering, 86(1), 295–306. https://doi.org/10.1016/j.ijimpeng.2015.08.014.

[64] Abtew, M. A., Boussu, F., & Bruniaux, P. (2021). Dynamic impact protective body armour: A comprehensive appraisal on panel engineering design and its prospective materials. Defence Technology, 17(6), 2027–2049. https://doi.org/10.1016/j.dt.2021.03.016.

[65] Hosur, M., Vaidya, U., Ulven, C., & Jeelani, S. (2003). Performance of stitched/unstitched woven carbon/epoxy composites under high velocity impact loading. Composite Structures, 64(3–4), 455–466. https://doi.org/10.1016/j.compstruct.2003.09.046.

[66] Islam and Muhammed Kamrul (2023). The Dynamic Response of Additively Manufactured Bioinspired Structures. 65(3), 555–566. https://doi.org/10.26190/unsworks/25262.

[67] Mohan, S., & Velu, S. (2013). Ballistic impact behaviour of unidirectional fibre reinforced composites. International Journal of Impact Engineering, 63, 164–176. https://doi.org/10.1016/j.ijimpeng.2013.07.008.

[68] Naik, N., & Shrirao, P. (2004). Composite structures under ballistic impact. Composite Structures, 66(1–4), 579–590. https://doi.org/10.1016/j.compstruct.2004.05.006.

[69] Saleem, I., Abed, M., & Ahmed, P. (2021). Numerical and experimental study of hybrid composite body armor. Engineering and Technology Journal, 39(11), 1681–1687. https://doi.org/10.30684/etj.v39i11.2274.

[70] Shaktivesh, N., Nair, N., Kumar, C. S., & Naik, N. (2013). Ballistic impact performance of composite targets. Materials & Design (1980-2015), 51, 833–846. https://doi.org/10.1016/j.matdes.2013.04.093.

[71] Shi, Y., Yan, T., Lai, W., Lu, D., & Lin, C. (2023). Fabric preparation of Stab-Resistant functional clothing. In Frontiers in artificial intelligence and applications, 51(2), 833–846. https://doi.org/10.3233/faia220714.

[72] Cichocka, A., Frydrych, I., Zawadzki, P., Kaczmarek, Ł., Irzmańska, E., & Kropidłowska, P. (2025). Basalt-Based Composite with Reduced Graphene Oxide (rGO)—Preliminary Study on Anti-Cut Properties. Materials, 18(24), 55-63. https://doi.org/10.3390/ma18245513.

[73] Zhang, X., Li, T., Wang, Z., Peng, H., Lou, C., & Lin, J. (2020). Facile fabrication and mass production of TPU/Silica/STF coated aramid fabric with excellent flexibility and quasi-static stab resistance for versatile protection. Progress in Organic Coatings, 151, 106-108. https://doi.org/10.1016/j.porgcoat.2020.106088.

[74] Lassandro, F., Sebastiano, M., Zei, F., & Bazzicalupo, P. (1994). The role of dityrosine formation in the crosslinking of CUT-2, the product of a second cuticlin gene of Caenorhabditis elegans. Molecular and Biochemical Parasitology, 65(1), 147–159. https://doi.org/10.1016/0166-6851(94)90123-6.

[75] Ioanna, T., & M. Amalia, M. (2023). Microplastic Particles in Sandy Beaches of Thessaloniki Gulf, Greece, WSEAS Transactions on Environment and Development, Vol. 19, 1380–1385. DOI: 10.37394/232015.2023.19.124.

APPENDIX

Table 1. A combination of Material properties collect from all following reference papers.

Brass		
Gruneisen coefficient	Shear modulus (Pa)	Density ($kg \cdot m^{-3}$)
2.04	4.6e + 010	8450

lead						
Density ($kg \cdot m-3$)	Specific heat constant pressure	Shear modulus (Pa)	Initial yield stress Y	Maximum yield stress Y	Hardening constant B	Hardening exponent n
11340	124	8.6e + 009	8e + 006	1e + 008	110	0.52

Fiber Cement			
Temperature, oC	Young's modulus (Pa)	Poisson's ratio	Bulk modulus (Pa)
25	7.62e + 009	0.1	3.175e + 009

Density ($kg \cdot m-3$)	Tensile ultimate strength (Pa)	Yield strength (Pa)	Tangent modulus (Pa)	Shear modulus (Pa)
1390	2.9e + 009	6e + 006	1.2e + 007	3.4636e + 009

Kevlar 29						
Temperatue (°C)	Young's modulus X direction (Pa)	Young's modulus Y direction (Pa)	Young's modulus Z direction (Pa)	Poisson's ratio XY	Density ($kg \cdot m^{-3}$)	Specific heat constant pressure $J \cdot kg-1 \cdot C-1$
25	1.85e + 010	1.85e + 010	6e + 009	0.25	1440	1420
Poisson's ratio YZ	Poisson's ratio XZ	Shear modulus XY (Pa)	Shear modulus YZ (Pa)	Shear modulus XZ (Pa)	Compressive yield strength (Pa)	Tensile yield strength (Pa)
0.33	0.33	7.7e + 008	5.43e + 009	5.43e + 009	1.85e + 008	1.85e + 009
Interlaminar normal strength (MPa)	Strain to failure in the warp direction	Strain to failure in the weft direction	Elastic modulus in the warp direction (GPa)	Elastic modulus in the weft direction, (GPa)	Through-thickness compressive modulus, (GPa)	Interlaminar shear strength, (MPa)
34.5	0.1	0.1	18.5	18.5	6	9

Kevalr 49				
Density ($kg\ m^{-3}$)	Tensile failure strength (s^{-1})	Failure strain (GPa)	Strain rate (%)	Cunniff velocity (ms^{-1})
1440	1350	3.08	3.86	650

Physical Parameters, Kevlar 29				
Property	Warp yarns/inch	Weft yarns/inch	Areal density (g/m^2)	Thickness (mm)
2D-P	40	32	363.75	0.64
3D-A	40	120	745.86	1.17
3D-O	40	120	780.36	1.24

Kavler 129				
Elastic modulus in the warp direction (GPa), E_1	Elastic modulus in the weft direction, E_2 (GPa)	Through-thickness compressive modulus, E_3 (GPa)	In-plane Poisson's ratio	Through-thickness Poisson's ratio
22	22	9	0.77	0.33

Density, ρ (g/cm^3)	Strain to failure in the warp direction, STF_1	Strain to failure in the weft direction, STF_2	Interlaminar normal strength,S_N (MPa)	Tensile strength in the warp direction, S_1 (MPa)
1.23	0.036	0.036	34.5	800.0
In-plane shear strength,S_{12} (MPa)	Through-thickness shear Strength, $S_{23,}$ S_{13} (MPa)	Tensile strength in the weft direction, S_2 (MPa)	Through-thickness compression strength (MPa)	
77	1000	800.0	1200	

Steel 1006			
Gruneisen coeffiffiffifficient	Initial yield stress Pa	Hardening constant Pa	Hardening exponent
2.17	3.5e + 008	2.75e + 008	0.36
Strain rate constant	Thermal softening exponent	Melting Temperature, ^oC	Reference strain rate, sec
2.2e − 002	1	1537.8	1

Polypropylene sheet		
Tenacity (gpd)	Strain (%)	Modulus (gpd)
17.93 (14.23)	4.08 (14.20)[1]	98.14 (19.18)

[1] The value in parentheses represents the coefficient of variation calculated from 15 individual readings for each sample.

Dyneema				
Density ($kg\ m^{-3}$)	Tensile failure strength (s^{-1})	Failure strain (GPa)	Strain rate (%)	Cunniff velocity (ms^{-1})
970	700	2.55	6.26	698

Spectra 900				
Density ($kg\ m^{-3}$)	Tensile failure strength (s^{-1})	Failure strain (GPa)	Strain rate (%)	Cunniff velocity (ms^{-1})
970	433	2.5	3	689

M5				
Density ($kg\ m^{-3}$)	Tensile failure strength (s^{-1})	Failure strain (GPa)	Strain rate (%)	Cunniff velocity (ms^{-1})
1700	Not stated	4	1.4	712

Toray T1000				
Density ($kg\ m^{-3}$)	Tensile failure strength (s^{-1})	Failure strain (GPa)	Strain rate (%)	Cunniff velocity (ms^{-1})
1800	Not stated	6.4	2.2	947

Toray T700				
Density ($kg\ m^{-3}$)	Tensile failure strength (s^{-1})	Failure strain (GPa)	Strain rate (%)	Cunniff velocity (ms^{-1})
1570	1000	3.4	1.57	665

Polypropylene (PP)		
Flexural modulus (MPa)	Flexural strength (MPa)	Strain at maximum stress (%)
2008	66.9	7.9

Epoxy		
Flexural modulus (MPa)	Flexural strength (MPa)	Strain at maximum stress (%)
3155	117.7	4.3

Twaron–PP		
Flexural modulus (MPa)	Flexural strength (MPa)	Strain at maximum stress (%)
1865	68.9	15.8

Twaron1–Epoxy

Flexural modulus (MPa)	Flexural strength (MPa)	Strain at maximum stress (%)
3038	117.8	6.9

Tungsten alloy						
Density (kg/m^3)	Young's Modulus (GPa)	Shear modulus (GPa)	Poison ratio	Static yield stress (MPa)	Strain hardening modulus (MPa)	Strain hardening exponent
17,600	314	122	0.29	1506	177	0.12
Strain rate coefficient	Thermal softening exponent	Initial reference temperature (K)	Melting temperature (K)	Slope in Us versus Up diagram	Gruneisen coefficient	Elastic wave speed (m/s)
0.016	1	300	1723	S1 = 1.23 S2 = S3 = 0	1.54	4029

99.5% Alumina				
Density (kg/m^3)	Shear modulus (GPa)	Intact strength coefficient	Fractured strength coefficient	Strain rate coefficient (s^{-1})
3700	90.16	0.93	0.31	0
Fractured strength exponent	Intact strength exponent	Normalized maximum fractured strength	Hugoniot elastic limit (MPa)	Pressure at Hugoniot elastic limit (MPa)
0.6	0.6	0.2	19,000	1460

Bulking factor	Elastic bulk modulus (MPa)	Coeff. For 2nd degree term in EOS (MPa)	Coeff. For 3rd degree term in EOS (MPa)	Damage coefficient	Damage exponent
1	130,950	0	0	0.005	1

Twaron CT1000 (1680 dtex/1000 filaments)				
Elastic modulus in the warp direction, (GPa)	Elastic modulus in the weft direction, (GPa)	Through-thickness compressive modulus, (GPa)	In-plane Poisson's ratio	Through-thickness Poisson's ratio
20.44	8.9	8.9	0.31	0.49

Density (g/cm^3)	In-plane shear modulus (MPa)	Through-thickness shear modulus, (GPa)	Bulk modulus (GPa)	Shear Strength (GPa)
1.23	1.64	3.03	20.4	0.34

Longitudinal tensile strength (GPa)	Transverse tensile strength (GPa)	Transverse compressive strength (GPa)	Non-linear parameters of shear Stress
1.145	0.13	0.65	0

High Molecular Weight Polyethylene (HMWPE)			
Failure strength (GPa)	Failure strain	Axial modulus (GPa)	Density (kg/m^3)
2.8-4.0	0.029-0.038	90-140	970-980

Aramid			
Failure strength (GPa)	Failure strain	Axial modulus (GPa)	Density (kg/m^3)
2.8-3.2	0.015-0.045	60-115	1390-1440

LCP			
Failure strength (GPa)	Failure strain	Axial modulus (GPa)	Density (kg/m^3)
2.7-2.9	0.033-0.035	64-66	1400-1420

PBO			
Failure strength (GPa)	Failure strain	Axial modulus (GPa)	Density (kg/m^3)
5.4-5.6	0.024-0.026	270-290	1540-1560

PIPD			
Failure strength (GPa)	Failure strain	Axial modulus (GPa)	Density (kg/m^3)
3.9-4.1	0.011-0.013	320-340	1690-1710
Nylon			
Failure strength (GPa)	Failure strain	Axial modulus (GPa)	Density (kg/m^3)
0.06-0.08	1.5-2.5	1.0-1.5	1070-1170
S-glass			
Failure strength (GPa)	Failure strain	Axial modulus (GPa)	Density (kg/m^3)
4.64-4.66	0.053-0.055	82-92	2470-2490

IRON-ARMCO					
Reference density (g/cm3)	Bulk modulus (kPa)	Reference temperature (K)	Specific heat capacity (J/kgK)	Strength : Johnson-Cook Shear modulus (kPa)	Yield Stress (kPa)
7.83	1.64E+07	300	451.99	8E+07	1.75E+05
Hardening exponent	Strain rate constant	Thermal softening exponent	Melting temperature (K)	Failure model	Hardening constant (kPa)
0.32	0.06	0.55	1811	None	3.8E+05

Carbon fiber (CF)				
Density ρ, (g/cm3)	E_{11} (GPa)	E_{22} (GPa)	E_{33} (GPa)	υ_{12}
1.406	8.6	28.8	28.8	0.07
υ_{23}	υ_{31}	G_{12} (GPa)	G_{23} (GPa)	G_{31} (GPa)
0.093	0.07	3.7	3.79	3.7

Glass Fiber (GF)				
Density ρ, (g/cm3)	E_{11} (GPa)	E_{22} (GPa)	E_{33} (GPa)	υ_{12}
2.0	13	40	40	0.057
υ_{23}	υ_{31}	G_{12} (GPa)	G_{23} (GPa)	G_{31} (GPa)
0.36	0.057	4.71	3.153	3.153

Source: [1], [2], [3], [4], [5], [6], [7], [8], [9], [10], [11], [12], [13], [14], [15], [16], [17], [18], [19], [20], [21], [22], [23], [24], [25], [26], [27], [28], [29], [30] ,[53], [54], [55], [56], [57], [58], [59], [66], [67], [68], [69], [70], [71], [72]

Table 2. Comparative Summary of Key Ballistic Armor Studies

Ref.	**Armor material / stacking**	**Projectile type**	**Velocity range (m/s)**	**Method**	**Performance metrics**	**Key findings**
[23]	Fiber cement / Kevlar-29 / steel backing	9 mm FMJ	~400	Exp + Sim (AUTODYN)	Penetration, deformation	≥1.5 mm steel backing required for BR2 protection
[24]	ZTA ceramic / Twaron-PP or Twaron-epoxy	7.62 mm AP	450–750	Exp + Sim (LS-DYNA)	Ballistic limit, BFS	Ceramic + Twaron-PP showed the highest energy absorption
[25]	B_4 C ceramic / UHMWPE	7.62 mm AP	~850	Exp + Sim (LS-DYNA)	Residual velocity, BFD	Ceramic–UHMWPE synergy reduced penetration effectively
[26]	Al_2 O_3 ceramic / Kevlar-epoxy	7.62 mm FMJ	~847	Exp + Sim (ABAQUS)	BFS, penetration depth	Ceramic front layer crucial for projectile blunting
[28]	SiC ceramic / UHMWPE	7.62 mm AP (WC core)	~930	Exp + Sim (LS-DYNA)	Penetration, BFD	Optimized thickness lowered weight with NIJ IV protection
[29]	B_4 C ceramic / HPPE-epoxy	7.62 mm AP (M61)	~850	Exp + Sim (ABAQUS)	DOP, stress distribution	Balanced ceramic–polymer design improved stopping power
[30]	Twaron-PP vs Twaron-epoxy	7.62 mm AP	~800	Experimental	Ballistic limit, failure mode	PP matrix outperformed epoxy due to higher ductility
[32]	3D carbon fiber / UHDP	9 mm FMJ	~430	Simulation	Velocity decay, BFD	Optimized stacking reduced backface deformation

Source: [23], [24], [25], [26], [28], [29], [30], [32]

Table 3. Simulation-Experiment Validation Trends Reported in Literature

Study Reference	**Solver / Tool**	**Materials Modeled**	**Experimental Validation Metrics**	**Validation Outcome Reported**
[23]	ANSYS AUTODYN	Fiber cement + Kevlar-29 + Steel	Deformation, penetration, layer failure	Simulation closely matched experimental deformation and penetration behavior
[24]	LS-DYNA	ZTA Ceramic + Twaron composites	Ballistic limit (BL), damage morphology	Numerical BL and failure modes consistent with ballistic tests
[25]	LS-DYNA	B_4 C + UHMWPE hybrid	Residual velocity, Back-face deformation (BFD), ceramic cracking	Good correlation between predicted and measured residual velocity and BFD
[26]	ABAQUS/Explicit	Al_2O_3 ceramic + Kevlar composite	Penetration depth, fiber damage, stress waves	Simulation reproduced penetration behavior and composite failure mechanisms.
[28]	AUTODYN (ANSYS)	Heat-treated armor steel	Depth of penetration (DOP), plate deformation	Simulation results validated against DMRL ballistic testing data
[29]	LS-DYNA	SiC ceramic + UHMWPE	Penetration, BFD, energy absorption	Numerical outputs showed strong agreement with test observations
[30]	ABAQUS/Explicit	B_4 C ceramic + HPPE composite	DOP, stress distribution, projectile arrest	Simulation predictions aligned with NIJ-standard experimental outcomes
[32]	LS-DYNA	SiC + Kevlar composite	Residual velocity, penetration, damage patterns	Experimental and simulated damage profiles matched closely
[23]	AUTODYN	Alumina + Kevlar–epoxy	Residual velocity, ceramic fragmentation	Validated model reproduced experimental ballistic resistance
[24]	LS-DYNA	Armor steel systems	Velocity decay, deformation, energy transfer	Simulation trends confirmed by high-speed experimental imaging
[25]	LS-DYNA	Aramid–epoxy laminates	Stress distribution, velocity reduction	Agreement between predicted and observed failure behavior
[26]	LS-DYNA	Transparent armor glass composites	Penetration depth, delamination	The model successfully predicted damage evolution under STANAG conditions
[28]	LS-DYNA	3D carbon fiber + UHDP	BFD, velocity decay	Numerical energy dissipation trends matched the literature experimental data

Source: [23], [24], [25], [26], [28], [29], [30], [32]

Contribution of Individual Authors to the Creation of a Scientific Article (Ghostwriting Policy)

- Shah Nusrat Jahan Shanta carried out the review paper analysis, performed the composing, analyzed the results, and prepared the initial draft of the manuscript.
- Abdus Sattar Mollah supervised the research work, provided technical guidance, reviewed the methodology, and revised the manuscript for important intellectual content.

Sources of Funding for Research Presented in a Scientific Article or Scientific Article Itself

This work was financially supported by the Military Institute of Science and Technology (MIST), which provided the necessary resources for conducting this study.

Conflict of Interest

The authors have no conflicts of interest to declare that are relevant to the content of this article.

Creative Commons Attribution License 4.0 (Attribution 4.0 International, CC BY 4.0)

This article is published under the terms of the Creative Commons Attribution License 4.0
https://creativecommons.org/licenses/by/4.0/deed.en_US